International Ocean Discovery Program

Expedition 379 Preliminary Report

Amundsen Sea West Antarctic Ice Sheet History

Development and sensitivity of the West Antarctic Ice Sheet tested from drill records of the Amundsen Sea Embayment

18 January–20 March 2019

Karsten Gohl, Julia S. Wellner, Adam Klaus, and the Expedition 379 Scientists

IODP
INTERNATIONAL OCEAN DISCOVERY PROGRAM

Publisher's notes

Core samples and the wider set of data from the science program covered in this report are under moratorium and accessible only to Science Party members until 23 August 2020.

This publication was prepared by the European Consortium for Ocean Research Drilling (ECORD) Science Operator (ESO) and Texas A&M University (TAMU) as an account of work performed under the International Ocean Discovery Program (IODP). Funding for IODP is provided by the following international partners:

National Science Foundation (NSF), United States
Ministry of Education, Culture, Sports, Science and Technology (MEXT), Japan
European Consortium for Ocean Research Drilling (ECORD)
Ministry of Science and Technology (MOST), People's Republic of China
Korea Institute of Geoscience and Mineral Resources (KIGAM)
Australia-New Zealand IODP Consortium (ANZIC)
Ministry of Earth Sciences (MoES), India
Coordination for Improvement of Higher Education Personnel (CAPES), Brazil

Portions of this work may have been published in whole or in part in other IODP documents or publications.

Disclaimer

Copyright

Citation

Gohl, K., Wellner, J.S., Klaus, A., and the Expedition 379 Scientists, 2019. *Expedition 379 Preliminary Report: Amundsen Sea West Antarctic Ice Sheet History.* International Ocean Discovery Program. https://doi.org/10.14379/iodp.pr.379.2019

ISSN
World Wide Web: 2372-9562

May 2019

Expedition 379 participants

Expedition 379 scientists

Karsten Gohl
Co-Chief Scientist
Department of Geosciences
Alfred Wegener Institute Helmholtz—Center for Polar and Marine Research
Germany
karsten.gohl@awi.de

Julia S. Wellner
Co-Chief Scientist
Earth & Atmospheric Sciences
University of Houston
USA
jwellner@uh.edu

Adam Klaus
Expedition Project Manager/Staff Scientist
International Ocean Discovery Program
Texas A&M University
USA
aklaus@iodp.tamu.edu

Thorsten Bauersachs
Organic Geochemist/Geomicrobiologist
Institute of Geosciences
Christian-Albrechts University
Germany
thorsten.bauersachs@ifg.uni-kiel.de

Steven M. Bohaty
Paleontologist (diatoms)
Ocean and Earth Science
National Oceanography Centre Southampton
University of Southampton
United Kingdom
S.Bohaty@noc.soton.ac.uk

Margot Courtillat
Paleontologist (foraminifers)
Centre of Education and Research on Mediterranean Environments (CEFREM) Laboratory
University of Perpignan
France
margot.courtillat@hotmail.com

Ellen A. Cowan
Sedimentologist
Department of Geological and Environmental Sciences
Appalachian State University
USA
cowanea@appstate.edu

Mariana S.R. Esteves
Sedimentologist
Centre for Arctic Gas Hydrate, Environment and Climate (CAGE)
The Arctic University of Norway—UiT
Norway
mariana.esteves@uit.no

Marcelo A. De Lira Mota
Palynologist
School of Geography, Earth and Environmental Sciences
University of Birmingham
United Kingdom

Also at:
Technological Institute of Micropaleontology
University of Vale do Rio dos Sinos (UNISINOS)
Brazil
mal546@bham.ac.uk

John M. Fegyveresi
Physical Properties/Downhole Measurements Specialist
Cold Regions Research and Engineering Laboratory (CRREL)
Engineer Research and Development Center, US Army Corps
USA
fegy.john@gmail.com

Thomas Frederichs
Paleomagnetist
Faculty of Geosciences
University of Bremen
Germany
frederichs@uni-bremen.de

Liang Gao
Paleomagnetist
School of the Earth Sciences and Resources
China University of Geosciences
China
lgao@cugb.edu.cn

Anna Ruth Halberstadt
Sedimentologist
Geosciences
University of Massachusetts-Amherst
USA
ahalberstadt@umass.edu

Claus-Dieter Hillenbrand
Sedimentologist
British Antarctic Survey
United Kingdom
hilc@bas.ac.uk

Keiji Horikawa
Sedimentologist
University of Toyama
Graduate School of Science and Engineering for Research
Japan
horikawa@sci.u-toyama.ac.jp

Masao Iwai
Paleontologist (diatoms)
Kochi University
Kochi Core Center (KCC)/Center for Advanced Marine Core Research
Japan
iwaim@kochi-u.ac.jp

Ji-Hoon Kim
Inorganic Geochemist
Petroleum and Marine Research Division
Korea Institute of Geoscience & Mineral Resources (KIGAM)
Republic of Korea
save@kigam.re.kr

Theresa M. King
Physical Properties/Downhole Measurement Specialist
College of Marine Science
University of South Florida
USA
theresaking@mail.usf.edu

Johann P. Klages
Sedimentologist
Alfred Wegener Institute Helmholtz—Center for Polar and Marine Research
Germany
johann.klages@awi.de

Sandra Passchier
Sedimentologist
Earth and Environmental Studies
Montclair State University
USA
passchiers@mail.montclair.edu

Michelle L. Penkrot
Physical Properties/Downhole Measurement Specialist
Department of Geological Sciences
University of Florida
USA
mpenkrot09@gmail.com

Joseph G. Prebble
Palynologist
Paleontology Department
GNS Science
New Zealand
j.prebble@gns.cri.nz

Waliur Rahaman
Inorganic Geochemist
Cryosphere and Climate
National Centre for Antarctic and Ocean Research (NCAOR)
India
waliur@ncaor.gov.in

Benedict T.I. Reinardy
Sedimentologist
Institutionen för Naturgeografi
Stockholm University
Sweden
benedict.reinardy@natgeo.su.se

Johan Renaudie
Paleontologist (radiolarians)
Museum fur Naturkunde
Leibniz-Institut fur Evolutions und Biodiversitätsforschung
Germany
johan.renaudie@mfn.berlin

Delaney E. Robinson
Sedimentologist
Earth & Atmospheric Sciences
University of Houston
USA
derobin3@central.uh.edu

Reed P. Scherer
Paleontologist (diatoms)
Geology and Environmental Geosciences
Northern Illinois University
USA
reed@niu.edu

Christine S. Siddoway
Sedimentologist
Department of Geology
Colorado College
USA
csiddoway@coloradocollege.edu

Li Wu
Sedimentologist
State Key Laboratory of Marine Geology
Tongji University
China
wuli@tongji.edu.cn
460743265@qq.com

Masako Yamane
Physical Properties/Downhole Measurement Specialist
Nagoya University
Institute for Space-Earth Environmental Research
Japan
yamane@nendai.nagoya-u.ac.jp

Outreach and education

Vivien Cumming
United Kingdom
viviencumming@gmail.com

Karen Romano Young
USA
wrenyoung@gmail.com

Ice observers

J. Garry N. MacCaull
Weather/Ice Observer
Canada

John L. Powell
Weather/Ice Observer
Canada

Operational and technical staff

SIEM Offshore AS officials

Jacob C. Robinson
Master of the Drilling Vessel

Mark Robinson
Drilling Supervisor

JRSO shipboard personnel and technical representatives

Elissa Barris
Marine Laboratory Specialist (temporary)

Susan Boehm
Marine Laboratory Specialist

Ty Cobb
Marine Laboratory Specialist

Aaron De Loach
Assistant Laboratory Officer

Tim Fulton
Senior Imaging Specialist

Clayton Furman
Logging Engineer

Randy Gjesvold
Marine Instrument Specialist

Sandra Herrmann
Assistant Laboratory Officer

Michael Hodge
Marine Computer Specialist

Jon Howell
Applications Developer

Rhonda Kappler
Publications Specialist

Nicolette Lawler
Marine Laboratory Specialist

Chang Liu
Marine Laboratory Specialist

Daniel Marone
Marine Laboratory Specialist

Aaron Mechler
Marine Laboratory Specialist

Michael Meiring
Drilling Engineer

Stephen Midgley
Operations Superintendent

William Mills
Laboratory Officer

Beth Ann Novak
Marine Laboratory Specialist

Catherine Smith
Curatorial Specialist

Steven Thomas
Marine Computer Specialist

Garrick Van Rensburg
Marine Instrumentation Specialist

Hai (James) Zhao
Applications Developer

Abstract

The Amundsen Sea sector of Antarctica has long been considered the most vulnerable part of the West Antarctic Ice Sheet (WAIS) because of the great water depth at the grounding line and the absence of substantial ice shelves. Glaciers in this configuration are thought to be susceptible to rapid or runaway retreat. Ice flowing into the Amundsen Sea Embayment is undergoing the most rapid changes of any sector of the Antarctic Ice Sheet outside the Antarctic Peninsula, including changes caused by substantial grounding-line retreat over recent decades, as observed from satellite data. Recent models suggest that a threshold leading to the collapse of WAIS in this sector may have been already crossed and that much of the ice sheet could be lost even under relatively moderate greenhouse gas emission scenarios.

Drill cores from the Amundsen Sea provide tests of several key questions about controls on ice sheet stability. The cores offer a direct record of glacial history offshore from a drainage basin that receives ice exclusively from the WAIS, which allows clear comparisons between the WAIS history and low-latitude climate records. Today, warm Circumpolar Deep Water (CDW) is impinging onto the Amundsen Sea shelf and causing melting of the underside of the WAIS in most places. Reconstructions of past CDW intrusions can assess the ties between warm water upwelling and large-scale changes in past grounding-line positions. Carrying out these reconstructions offshore from the drainage basin that currently has the most substantial negative mass balance of ice anywhere in Antarctica is thus of prime interest to future predictions.

The scientific objectives for this expedition are built on hypotheses about WAIS dynamics and related paleoenvironmental and paleoclimatic conditions. The main objectives are

1. To test the hypothesis that WAIS collapses occurred during the Neogene and Quaternary and, if so, when and under which environmental conditions;
2. To obtain ice-proximal records of ice sheet dynamics in the Amundsen Sea that correlate with global records of ice-volume changes and proxy records for atmospheric and ocean temperatures;
3. To study the stability of a marine-based WAIS margin and how warm deep-water incursions control its position on the shelf;
4. To find evidence for earliest major grounded WAIS advances onto the middle and outer shelf;
5. To test the hypothesis that the first major WAIS growth was related to the uplift of the Marie Byrd Land dome.

International Ocean Discovery Program (IODP) Expedition 379 completed two very successful drill sites on the continental rise of the Amundsen Sea. Site U1532 is located on a large sediment drift, now called Resolution Drift, and penetrated to 794 m with 90% recovery. We collected almost-continuous cores from the Pleistocene through the Pliocene and into the late Miocene. At Site U1533, we drilled 383 m (70% recovery) into the more condensed sequence at the lower flank of the same sediment drift. The cores of both sites contain unique records that will enable study of the cyclicity of ice sheet advance and retreat processes as well as bottom-water circulation and water mass changes. In particular, Site U1532 revealed a sequence of Pliocene sediments with an excellent paleomagnetic record for high-resolution climate change studies of the previously sparsely sampled Pacific sector of the West Antarctic margin.

Despite the drilling success at these sites, the overall expedition experienced three unexpected difficulties that affected many of the scientific objectives:

1. The extensive sea ice on the continental shelf prevented us from drilling any of the proposed shelf sites.
2. The drill sites on the continental rise were in the path of numerous icebergs of various sizes that frequently forced us to pause drilling or leave the hole entirely as they approached the ship. The overall downtime caused by approaching icebergs was 50% of our time spent on site.
3. An unfortunate injury to a member of the ship's crew cut the expedition short by one week.

Recovery of core on the continental rise at Sites U1532 and U1533 cannot be used to precisely indicate the position of ice or retreat of the ice sheet on the shelf. However, these sediments contained in the cores offer a range of clues about past WAIS extent and retreat. At Sites U1532 and U1533, coarse-grained sediments interpreted to be ice-rafted debris (IRD) were identified throughout all recovered time periods. A dominant feature of the cores is recorded by lithofacies cyclicity, which is interpreted to represent relatively warmer periods variably characterized by higher microfossil abundance, greater bioturbation, and higher counts of IRD alternating with colder periods characterized by dominantly gray laminated terrigenous muds. Initial comparison of these cycles to published records from the region suggests that the units interpreted as records of warmer time intervals in the core tie to interglacial periods and the units interpreted as deposits of colder periods tie to glacial periods.

The cores from the two drill sites recovered sediments of purely terrigenous origin intercalated or mixed with pelagic or hemipelagic deposits. In particular, Site U1533, which is located near a deep-sea channel originating from the continental slope, contains graded sands and gravel transported downslope from the shelf to the abyssal plain. The channel is likely the path of such sediments transported downslope by turbidity currents or other sediment-gravity flows. The association of lithologic facies at both sites predominantly reflects the interplay of downslope and contouritic sediment supply with occasional input of more pelagic sediment. Despite the lack of cores from the shelf, our records from the continental rise reveal the timing of glacial advances across the shelf and thus the existence of a continent-wide ice sheet in West Antarctica at least during longer time periods since the late Miocene.

Cores from both sites contain abundant coarse-grained sediments and clasts of plutonic origin transported either by downslope processes or by ice rafting. If detailed provenance studies confirm our preliminary assessment that the origin of these samples is from the plutonic bedrock of Marie Byrd Land, their thermochronological record will potentially reveal timing and rates of denudation and erosion linked to crustal uplift. The chronostratigraphy of both sites enables the generation of a seismic sequence stratigraphy not only for the Amundsen Sea rise but also for the western Amundsen Sea along the Marie Byrd Land margin through a connecting network of seismic lines.

Introduction

For decades, the ice in the drainage basins flowing into the Amundsen Sea has been considered the most vulnerable part of the

West Antarctic Ice Sheet (WAIS) because of the great water depth at the grounding line and the lack of substantial buttressing ice shelves (Hughes, 1981). Glaciers in this configuration are thought to be susceptible to rapid or runaway retreat (Schoof, 2007). Ice flowing into the Amundsen Sea Embayment is undergoing the most rapid changes of any sector of the Antarctic Ice Sheet, including changes caused by substantial grounding line retreat over recent decades, as observed from satellite data (Milillo et al., 2019). Recent models suggest that a threshold leading to the collapse of WAIS in this sector may have been passed already (Joughin et al., 2014) and that much of the ice sheet could be lost even under relatively moderate greenhouse gas emission scenarios (DeConto and Pollard, 2016). Model projections are limited by lack of constraints in several areas, most notably in a lack of detailed reconstructions of glacial history.

Drill cores from the Amundsen Sea (Figure **F1**) provide tests of several key questions about controls on ice sheet stability. First, the cores offer a direct record of glacial history in a drainage basin that receives ice only from the WAIS and thus allow clear comparisons between the WAIS history and low-latitude climate records. Ice draining into the Amundsen Sea is grounded below sea level and thus allows a test of the marine ice sheet instability theory through correlation of the ice sheet history to sea level changes. Although there are currently only relatively small ice shelves in front of the grounding line today, during some points of its history the embayment had more extended ice shelves (Kirshner et al., 2012; Klages et al., 2017) that allow examination of the grounding-line history relative to the ice-shelf history. Today, warm Circumpolar Deep Water (CDW) impinges onto the Amundsen Sea shelf, which causes melting of the underside of the ice in some places (Milillo et al., 2019). Reconstructions of past CDW intrusions (Hillenbrand et al., 2017; Minzoni et al., 2017) can assess the ties between warm water and large-scale changes in past grounding-line positions. Carrying out these reconstructions offshore from the drainage basin that currently has the largest negative mass balance of ice of anywhere in Antarctica (Paolo et al., 2015) is thus of prime interest to future predictions. Finally, Expedition 379 is part of a suite of Antarctic International Ocean Discovery Program (IODP) expeditions that allow large-scale reconstructions and comparisons between different drainage basins.

Background

The fourth assessment report of the Intergovernmental Panel on Climate Change (IPCC) (2007) highlighted the fact that the response of continental ice sheets to climatic changes and their contribution to global sea level change is the largest unknown variable in predicting future sea level change. The fifth and latest assessment report of the IPCC (2013) includes more information about the likely contributions to sea level change from the Antarctic, but these contributions remain one of the primary unknowns in predictions of future change. Also, the 2013 IPCC assessment report emphasizes that if there is a substantial increase in the rate of sea level rise in the next century, it is likely to come from marine-based ice like that in the Amundsen Sea Embayment. The recent special report of the IPCC (2018) concludes that marine ice sheet instability in Antarctica and the irreversible loss of the Greenland ice sheet could be triggered by ~1.5° to 2°C of global warming and could result in multimeter sea level rise over hundreds to thousands of years.

The WAIS rests on a continental shelf that typically deepens toward the interior of the Antarctic continent. This fore-deepened continental shelf, and thus the base of the ice, is mostly below sea level. Therefore, the marine-based WAIS is sensitive to global sea level rise and regional oceanographic and atmospheric changes, and its history has been highly dynamic (e.g., Joughin and Alley, 2011). A complete WAIS collapse would raise the global sea level by 3.3 to 4.3 m (Fretwell et al., 2013), whereas the collapse of its Amundsen Sea drainage sector would raise the sea level by ~1.5 m (Vaughan, 2008). Over the most recent decades, glaciers draining into the Amundsen Sea thinned at a rapid rate, their flow speed dramatically increased, and their grounding lines retreated significantly, thereby contributing to present sea level rise at a faster rate than from any other glacier on Earth (e.g., Joughin and Alley, 2011; Joughin et al., 2012; Paolo et al., 2015; Rignot et al., 2019).

The present ice loss in the Amundsen Sea region is mainly attributed to sub–ice shelf melting induced by relatively warm CDW upwelling onto the shelf and spreading through deep bathymetric troughs toward the grounding zones (e.g., Arneborg et al., 2012; Joughin et al., 2012). It is unclear, however, whether the current ice loss results from recent climatic/oceanographic warming or recent internal ice sheet dynamics (Joughin and Alley, 2011; Joughin et al., 2012). If the WAIS has undergone similar thinning and retreat in the past, the factors driving that retreat can be compared to modern conditions.

The reconstruction and quantification of WAIS collapse during the Neogene and Quaternary will provide constraints for ice sheet models (Figure **F2**) that predict future WAIS behavior and resulting sea level rise. Numerous modeling studies have tried to link the waxing and waning of the WAIS to various forcing mechanisms (e.g., Pollard and DeConto, 2009; Holden et al., 2010; DeConto and Pollard, 2016; Sutter et al., 2016). However, large uncertainties exist regarding the spatial and temporal variability of past ice sheet advance and retreat. These uncertainties are mainly caused by the lack of data from cores drilled proximal to the WAIS. The only existing drill cores along the Pacific Antarctic margin outside the Ross Sea are from Deep Sea Drilling Project (DSDP) Leg 35 in the Bellingshausen Sea (Hollister and Craddock, 1976) and Ocean Drilling Program (ODP) Leg 178 on the Antarctic Peninsula margin (Barker and Camerlenghi, 2002). Results from Leg 178 Site 1097, drilled on the shelf, revealed a significant late Miocene change in sequence geometry on the outer shelf that may indicate a change in the typical extent of glacial advances, the dynamic behavior of ice streams, or glacial sediment transport (Barker and Camerlenghi, 2002; Bart et al., 2005; Larter et al., 1997). Scheuer et al. (2006a, 2006b) was able to correlate seismic horizons with Leg 178 Sites 1095 and 1096 on the continental rise and interpreted transitions from preglacial to intermediate- and full-glacial conditions from the eastern Bellingshausen Sea to the Amundsen Sea.

The most detailed results on Neogene WAIS history stem from the Antarctic Geological Drilling (ANDRILL) project in the western Ross Sea, which recovered early Miocene (~20 Ma) to Quaternary sequences in Cores AND-1B (Naish et al., 2009) and AND-2A (Passchier et al., 2011). Pliocene data from Core AND-1B indicate that orbitally induced oscillations of the WAIS resulted in transitions from grounded ice or ice shelves to open-water conditions (Naish et al., 2009; McKay et al., 2012). However, previous seismic stratigraphic work on the Ross Sea shelf beyond Site AND-1B revealed only seven shelf-wide grounding events (Alonso et al., 1992). Given the location of Site AND-1B, which is in a position to be overridden by both the East Antarctic Ice Sheet (EAIS) and the WAIS, the ANDRILL results are probably not representative of the WAIS outlets in the Amundsen, Bellingshausen, and Weddell Seas. Sedimentary records from the Ross and Weddell Seas provide only an integrated archive of WAIS and EAIS dynamics, whereas records from the Amundsen Sea will provide an unambiguous WAIS signal. We expect that results from recent IODP Expedition 374 to the Ross Sea shelf and slope will provide further insight into the WAIS dynamics for the Ross Sea sector. Although the Filchner-Ronne Ice Shelf extends far into the southern Weddell Sea, making grounding-line proximal positions difficult to access, only small and narrow ice shelves exist in the Amundsen Sea Embayment today.

Oceanographic setting

Persistent sea ice cover characterizes Pine Island Bay and the Amundsen Sea Embayment (e.g., Jacobs et al., 2012), and although sea ice cover has decreased significantly in recent decades (Parkinson and Cavalieri, 2012), 2018 and 2019 did not follow this trend; the sea ice cover of the Amundsen Sea was extensive throughout the entire austral summer and fall. Very little data on tidal ranges exist for the Amundsen Sea, but models suggest a 40 cm tidal height, making the area microtidal (Padman et al., 2002). Water mass temperatures within Pine Island Bay typically range between −1.5° and 0°C. The exception to this is warm CDW, which can reach 1.5°C and impinges onto the shelf through deep glacially carved troughs (Walker et al., 2007; Jacobs et al., 2011, 2013) and at times reaches into some of the smaller bays and fjords on the inner shelf (Minzoni et al., 2017). Productivity in the Amundsen Sea is among the highest in the Southern Ocean and includes phytoplankton blooms related to polynyas (Arrigo et al., 2008; Minzoni et al., 2017). CDW is widely considered to be the primary external driver of contemporary glacier retreat in the Amundsen Sea, and recent work has shown that it can vary on seasonal (Kim et al., 2017) to decadal (Jenkins et al., 2016) timescales in response to wind stress at the continental shelf edge.

Geological setting

Together, ice sheet dynamics and tectonic as well as other geologic processes have shaped the Amundsen Sea continental shelf and rise. A 500–700 m deep shelf is incised by two major paleo–ice stream troughs (Pine Island and Dotson-Getz) whose tributaries originate from ice-stream/glaciers on the innermost ultradeep (as deep as 1600 meters below sea level [mbsl]) shelf and converge at the transition from the inner to middle shelf. Both troughs extend toward the outer shelf, thereby becoming shallower and wider. The shelf geometry consists of a large pre- and synrift basin on the midshelf between the basement cropping out on the inner shelf and the buried basement highs on the outer shelf. A subordinate basin within the large midshelf basin may be associated with motion along an early West Antarctic Rift System branch. At least 4 km of preglacial strata were eroded by ice from the present inner shelf and coastal hinterland. At least five major erosional unconformities indicate phases of significant WAIS advances. Prograding sequences and subglacial bedforms on the outer shelf, subglacial tills recovered in cores, and radiocarbon dates on calcareous microfossils and organic matter in overlying sediments indicate that ground ice expanded to the outer shelf during the LGM and earlier glacial periods.

The continental rise is dominated by thick sedimentary deposition centers and by sediment drifts, both of which indicate strong bottom-current activity. Seismic data analysis from the Amundsen Sea rise reveals that sediment drift formation began in the Eocene/Oligocene (Uenzelmann-Neben and Gohl, 2012, 2014) (Figure **F3**). This observation indicates bottom-current activity and hence a cold climate for the late Paleogene in the area that today probably lies under the influence of Antarctic Bottom Water originating in the Ross Sea. Seismic records from the continental rise along the entire Marie Byrd Land margin mark the base of the sediment drifts throughout the Amundsen Sea and into the Ross Sea (Lindeque et al., 2016a, 2016b). These records provide insight into the sedimentation processes from preglacial to glacial times, variations in bottom-water circulation, early ice sheet growth, and glacial intensification toward the present icehouse regime (Uenzelmann-Neben and Gohl, 2012, 2014). However, stratigraphic age estimates are derived from long-distance seismic correlation with the western Antarctic Peninsula margin and the Ross Sea margin and hamper this insight.

Seismic records from the Amundsen Sea shelf show dipping strata of the midshelf that are possibly of Cretaceous to Miocene age and buried by aggradational, less consolidated strata of presumed Pliocene–Pleistocene age (Lowe and Anderson, 2002; Gohl et al., 2013b). Preliminary results from a seabed drilling expedition place constraints on the Cretaceous sequences on top of the outcropping bedrock of the middle to inner shelf of Pine Island Bay (Gohl et al., 2017). Since the mid-Miocene, the outer shelf and slope have undergone first progradational and then aggradational deposition (Nitsche et al., 1997; Hochmuth and Gohl, 2013; Gohl et al., 2013b). Several unconformities that possibly indicate phases of subglacial erosion and ice advance separate the dipping strata. Although most of the inner Amundsen Sea shelf is void of significant sedimentary cover (Lowe and Anderson, 2002; Graham et al., 2009; Gohl et al., 2013a, 2013b), a few small, shallow basins lie along its eastern border (Uenzelmann-Neben et al., 2007) and in front of Pine Island Glacier (Nitsche et al., 2013; Muto et al., 2016).

A bathymetric and structural high (Nitsche et al., 2007; Gohl et al., 2013b) separates the eastern and western Amundsen Sea continental shelves. Oceanward-dipping midshelf strata north of the outcropping basement are evident in seismic data from the Dotson-Getz Trough (Wellner et al., 2001; Graham et al., 2009; Weigelt et al., 2009; Gohl et al., 2013b) and exhibit alternating sequences of low and high reflectivity that are interpreted to be Miocene episodes of ice sheet advance and retreat. The glacial sequence stratigraphic model by Powell and Cooper (2002) proposed that glacial advances develop morainal banks consisting of unstratified diamicton, sand, and gravel that lead to a chaotic or semitransparent seismic reflection pattern. In contrast, stratified muds are deposited during a glacial retreat, which is expressed in seismic profiles as a succession of closely spaced continuous reflectors. Boundaries between the acoustic units are sharp, but without drilling, the timing of ice sheet oscillations remains unconstrained. Similar seismic facies occur on the Ross Sea and Antarctic Peninsula shelves, where drill cores confirmed that the chaotic/transparent units correspond to massive diamicton and acoustically stratified seismic facies correspond to distal glacimarine sediments (Anderson and Bartek, 1992; Bart and Anderson, 2000; Eyles et al., 2001).

The current seismostratigraphic model of the Amundsen Sea shelf was developed by long-distance correlation of seismic data with those of the Ross Sea shelf, which show striking similarities (Gohl et al., 2013b). Adopting the ages of the seismostratigraphic units and unconformities on the Ross Sea shelf, which are relatively well constrained by DSDP Leg 28 and ANDRILL records (e.g., De Santis et al., 1999; McKay et al., 2009), the shelf-basin formation model for the Amundsen Sea shows development from a Cretaceous synrift basin to glacially dominated strata in the Neogene and Quaternary (Gohl et al., 2013b). The seismostratigraphic record from the continental shelf is consistent with records from the Ross Sea (Bartek et al., 1991; Chow and Bart, 2003) and James Ross Basin in the northwestern Weddell Sea (Smith and Anderson, 2010), indicating a Miocene intensification of glaciation (De Santis et al., 1997) in accordance with findings from Core AND-2A (Warny et al., 2009; Passchier et al., 2011) and the Shallow Scientific Drilling on the Antarctic Continental Margin (SHALDRIL)-II drill cores (Anderson et al., 2011; Anderson and Wellner, 2011).

Apart from ice sheet dynamics inferred from the geometries and acoustic facies of seismic reflections, the ice-drainage pattern in the Amundsen Sea at the LGM and its substrate control were investigated by the analysis of sub- and proglacial bedforms visible in swath bathymetry surveys and acoustic subbottom profiler data (e.g., Larter et al., 2009). The subglacial bedforms on the shelf indicate that grounded ice expanded to the outer shelf or even the shelf edge during the recent past (Wellner et al., 2001; Lowe and Anderson, 2002; Graham et al., 2009, 2010; Jakobsson et al., 2012; Nitsche et al., 2013). Analysis of subglacial and glacimarine sediments recovered in cores from the continental shelf confirmed an LGM age for the last WAIS advance, allowed a reconstruction of its retreat history (Lowe and Anderson, 2002; Smith et al., 2011, 2014; Kirshner et al., 2012; Hillenbrand et al., 2013; Larter et al., 2014), and indicated dynamically evolving drainage systems (Ehrmann et al., 2011). Recently, studies of benthic foraminiferal assemblages (Minzoni et al., 2017) and the chemical composition (i.e., stable carbon isotopes and magnesium/calcium ratios) of benthic and planktonic foraminifer shells in ice-proximal marine sediments from the inner shelf (Hillenbrand et al., 2017) showed that variable inflow of CDW was the primary driver for grounding-line retreat along the coast of the Amundsen Sea Embayment throughout the Holocene and since the 1940s. Sedimentary sequences from the Amundsen Sea continental slope and rise spanning glacial–interglacial cycles to 1.8 Ma were investigated by multiproxy analyses to find evidence for or against a WAIS collapse during the Quaternary (Hillenbrand et al., 2002, 2009; Konfirst et al., 2012), as was previously suggested (e.g., Scherer et al., 1998; Scherer, 2003). One of these studies found a mid-Pleistocene depositional anomaly that may indicate a WAIS collapse between 621 and 478 ky ago (Hillenbrand et al., 2009). All of these studies provide a robust sedimentological framework for interpreting drill cores.

Objectives

The scientific goals and plan for this expedition are built on five hypotheses about WAIS dynamics and related paleoenvironmental and paleoclimatic conditions.

Hypothesis H1: the WAIS responded to atmospheric and oceanic warming by a major retreat from the shelf or by even partial to full collapse.

Ice sheet models hypothesize that past climate warming caused significant deglaciation of the WAIS (e.g., DeConto and Pollard, 2016). For instance, during the early middle Pliocene, Earth's climate was ~3°C warmer than at present (e.g., Haywood et al., 2009) and thus as warm as predicted for the end of this century, although atmospheric pCO_2 was ~400 ppm and other climatic boundary conditions were similar to the present (Pagani et al., 2010). The reasons for such a high atmospheric temperature during a time with modest greenhouse-gas forcing are still unknown. Results from Core AND-1B suggest repeated WAIS collapses during warm early middle Pliocene and Pleistocene interglacials (e.g., during Marine Isotope Stage [MIS] 31) (Naish et al., 2009; Pollard and DeConto, 2009; McKay et al., 2012; Villa et al., 2012). The hypothesis of WAIS collapses needs confirmation with a less ambiguous record from an outlet drainage basin exclusively affected by the WAIS. In drill cores from the Amundsen Sea margin, WAIS collapses would be recognizable by biogenic sedimentary sequences deposited during times with permanent open-water conditions and reduced supply of glacigenic debris from the West Antarctic hinterland similar to those documented in the Core AND-1B record (Naish et al., 2009). Such sediments would contain abundant microfossils and probably tephra layers from the Marie Byrd Land volcanic province (e.g., Le Masurier and Rex, 1991; Wilch et al., 1999), which are essential for dating the sediments and reconstructing paleoenvironmental conditions in the region. Thus, the cores will help to answer the crucial question: did the WAIS collapse during the Neogene and Quaternary, as previously suggested, and if yes, when and under which environmental conditions?

Hypothesis H2: ice-proximal records of ice sheet dynamics in the Amundsen Sea correlate with global records of ice-volume changes and proxy records for atmospheric and ocean temperatures.

The post-LGM retreat of the WAIS from the Amundsen Sea shelf was episodic (e.g., Lowe and Anderson, 2002; Graham et al., 2009, 2010; Jakobsson et al., 2012; Larter et al., 2014). The retreat episodes were likely triggered by different processes, including sea level rise, sub–ice shelf erosion by warm deep-water advection, destabilization of the ice sheet by subglacial meltwater outbursts, and grounding-line retreat into overdeepened inner-shelf basins (Jakobsson et al., 2011; Smith et al., 2011, 2014; Kirshner et al., 2012; Hillenbrand et al., 2013, 2017). These observations raise questions concerning the linkage between climate and glaciological forcing in regulating WAIS deglaciation. Throughout the Cenozoic era, unexplained discrepancies are observed between Earth's temperature and global ice volume reconstructed from proxies in deep-sea sediments, climate models, sea level estimates, and ice cores for the last 800 ky. Reexamination of previously studied cores highlights ongoing uncertainty about the timing of early ice sheet growth (Carter et al., 2017). The results of the Core AND-1B record (Naish et al., 2009) and Integrated Ocean Drilling Program Expedition 318 to the Wilkes Land margin (Cook et al., 2013) reignited the debate as to whether the Antarctic ice sheets underwent major collapses during Pliocene interglacials. Such collapses are neither directly recognizable from oxygen isotope proxies at far-field sites nor confirmed by the apparently persistent glaciation of the Antarctic Peninsula since the latest Miocene (Smellie et al., 2009) and repeated Pliocene ice sheet advances across the shelf that are observed in seismic profiles all along the Antarctic margin (e.g., Larter et al., 1997; Nitsche et al., 1997; Bart and Anderson, 2000; Smith and Anderson, 2010; Bart, 2001). Indeed, results from SHALDRIL cores and other data from the eastern Antarctic Peninsula shelf indicate gradual cooling and an associated decline in vegetation over the past 37 My culminating in early Pliocene ice sheet expansion onto the continental shelf (Anderson et al., 2011). Results from ODP Leg 178 cores from the western Antarctic Peninsula margin are consistent with repeated ice sheet advances throughout the Pliocene (Eyles et al., 2001; Hillenbrand and Ehrmann, 2005; Hepp et al., 2006; Bart, 2001) but also indicate significant oceanic warming during Pliocene interglacials (Hillenbrand and Cortese, 2006; Escutia et al., 2009; Hepp et al., 2009; Bart and Iwai, 2012). Expedition 379 drill sites will help us decipher whether the WAIS responded directly to the orbitally paced climatic cycles of the Pliocene and Quaternary or varied at periods determined by its internal dynamics, as findings from Leg 178 suggest for the Antarctic Peninsula Ice Sheet (Barker and Camerlenghi, 2002). Similar to cores from the Ross Sea and Antarctic Peninsula shelves (Eyles et al., 2001; McKay et al., 2009), the Leg 178 cores are incomplete because of glacial erosional unconformities. During Expedition 379, cores were drilled from deep-sea drifts on the continental rise of the Amundsen Sea Embayment to obtain complete sedimentary sequences. Similar drift sediments drilled on the western Antarctic Peninsula continental rise during Leg 178 provided excellent archives of Neogene to Quaternary ice sheet dynamics and paleoenvironmental changes (e.g., Hillenbrand and Ehrmann, 2005; Cowan et al., 2008; Hepp et al., 2006, 2009; Escutia et al., 2009; Bart and Iwai, 2012). A comparable potential has already been demonstrated for Pleistocene drift sediments recovered from the Amundsen Sea continental rise (Hillenbrand et al., 2009).

Hypothesis H3: the stability of marine-based WAIS margins is and has been controlled by warm deep-water incursions onto the shelf.

In model experiments, incursions of relatively warm CDW onto the West Antarctic continental shelf have been implicated in regulating WAIS behavior on orbital and suborbital timescales (Thoma et al., 2008; Pollard and DeConto, 2009; Jenkins et al., 2016). Therefore, records of past CDW upwelling are urgently needed to understand the relationship between WAIS dynamics and ocean circulation. Generating proxy records of past CDW incursions from marine sediment cores is still a challenge but was recently demonstrated to be possible in sediments from the Amundsen Sea Embayment shelf (Hillenbrand et al., 2017; Minzoni et al., 2017). With recent observations of present CDW advection predominantly through the paleo–ice stream troughs of the Amundsen Sea (e.g., Arneborg et al., 2012), drilling on the continental shelf has a good chance to recover sample material suitable for applying benthic foraminifer–based and other proxies to reconstruct past CDW upwelling onto the shelf and its effect on WAIS dynamics.

Hypothesis H4: major WAIS advances onto the middle and outer shelf have occurred since the middle Miocene.

Seismic data revealed progradational and aggradational deposition on the outer shelf and slope of the Amundsen Sea probably since the mid-Miocene (e.g., Nitsche et al., 1997, 2000; Hochmuth and Gohl, 2013; Gohl et al., 2013b). Numerous unconformities within strata on the shelf document frequent advance and retreat of grounded ice from the late Miocene until the Pliocene/Pleistocene, according to the stratigraphic age model by Gohl et al. (2013b). The preservation of buried grounding-zone wedges in the Pliocene/Pleistocene sequence on the outer Amundsen Sea shelf is consistent with the prolonged continuous accumulation of marine and glacimarine sediments in an open-marine setting, probably during a long interglacial period with a significantly reduced WAIS, as observed on the Ross Sea shelf during the early Pliocene. However, the models of grounded-ice advance and retreat across the Amundsen Sea shelf are based on long-distance correlations of seismic facies and characteristics, which are tested by core data to constrain past WAIS extent.

Hypothesis H5: the first WAIS advance onto the inner Amundsen Sea continental shelf occurred during the Oligocene and was related to the uplift of Marie Byrd Land.

The onset of major glaciation in West Antarctica is still not dated because of sparse drill cores. Records of IRD suggest that glaciers must have reached the coast of the Ross Sea in the early to mid-Oligocene (Miller et al., 2008). Ice sheet models (e.g., DeConto and Pollard, 2003) reconstructed an early WAIS nucleus in the mountain chain extending from elevated Marie Byrd Land over the Ellsworth Mountains to the southern Antarctic Peninsula. The exhumation and erosion history of Marie Byrd Land and especially the Marie Byrd Land dome is essential for the interrelations between ice sheet and lithosphere dynamics (e.g., Rocchi et al., 2006; Wilson and Luyendyk, 2009; Wilson et al., 2012, 2013; Spiegel et al., 2016) because (1) exhumation and erosion change topography, which in turn influences glacier movements by slope steepness; (2) exhumation is often associated with surface uplift, and high altitude favors formation of glaciers; and (3) glaciation changes erosion rates and, because of isostatic adjustment, exhumation rates. This relationship is investigated using detailed provenance and thermochronological analyses of Neogene drill samples from the midshelf and existing rock samples from the hinterland.

Operations plan/drilling strategy

The primary aim of our drilling campaign was to obtain core and log data from seaward-dipping strata along a transect from the Paleogene sequences close to the boundary with bedrock on the inner shelf to the Pliocene to Pleistocene sequences on the outer shelf and continuing onto the continental rise for continuous high-resolution records. Because sea ice conditions during the drilling expedition were unsuitable for accessing either the priority sites in Pine Island Trough or the transect targeting strata of comparable age and cross-shelf position in the Dotson-Getz Trough, a paleo–ice stream trough of the western Amundsen Sea Embayment, we drilled our third-tier priority sites on the continental rise. The sites we drilled during Expedition 379 were added to the proposal following the record sea ice in the 2017/2018 austral summer. The two sites (U1532 and U1533) were not lower in priority than other rise sites; instead, they were added to the proposal in 2018 when sites were no longer required to be on a crossing seismic line. This change provided an opportunity for alternates even farther north, and thus farther from likely sea ice cover than the originally proposed sites. Additional modifications in 2018 to our original proposal included approval of “ribbons” along the seismic line that allowed holes to be drilled in a range of positions and for maximum flexibility in severe ice conditions.

Our plan was to core two holes at each drill site using the advanced piston corer (APC), half-length advanced piston corer (HLAPC), and extended core barrel (XCB) system in the first hole and the rotary core barrel (RCB) system in the second hole and then collect log data in the deeper RCB hole. In reality, each of our two drill sites included far more holes than intended. Site U1532 includes seven holes, and Site U1533 has four holes. No holes were terminated by reaching target depths; we terminated the first 10 holes because of approaching icebergs, and we had to abandon the final hole because of an emergency medical evacuation.

The coring strategy at each site generally followed the operational plans; however, it was spread out over multiple holes. When we were forced to leave a hole, we drilled a new hole without coring through the upper section, and then coring resumed with some overlap. We initiated new holes following a standard offset of 20 m except when ice conditions would not allow a new hole close to the original site and other positions along the permitted ribbon were open. Thus, the holes at each site are more spread out than those of many other IODP expeditions.

Although downhole logging was planned for each site, no downhole log data were collected during Expedition 379 because of the premature termination of each hole.

Site summaries

Site U1532

Background

Site U1532 (proposed Site ASRE-08A) is located on the western upper flank of a large sediment drift (Resolution Drift) on the continental rise, 270 km north of the Amundsen Sea Embayment shelf edge (Figures **F1**, **F4**). This drill site was chosen as the first Expedition 379 site upon arriving in the Amundsen Sea because the sea ice distribution did not allow drilling at any of the other primary or alternate sites at that time. The Resolution Drift belongs to a system of five parallel sediment drifts on this rise that are characterized by gentle western and steep eastern flanks. Sediment drifts are commonly formed by deposition of suspended sediments transported by ocean-bottom contour currents. Deep-sea channels that originate at the foot of the continental slope and reach far into the abyssal plain separate the sediment drifts in the Amundsen Sea. Sediment is transported downslope through these channels by turbidity currents, slumps, and other gravity-driven processes that supply a large portion of the detritus deposited in the drifts (Nitsche et al., 2000; Dowdeswell et al., 2006). Sedimentation rates of drift deposits along the Antarctic margin are extremely high, which makes them high-priority drill targets to obtain continuous paleoceanographic and paleo–ice sheet records of high temporal resolution (Uenzelmann-Neben and Gohl, 2012). Stratigraphic interpretations of seismic lines across the sediment drifts of the Amundsen Sea (e.g., Nitsche et al., 2000; Scheuer et al., 2006b; Uenzelmann-Neben and Gohl, 2012, 2014) are so far only constrained by long-distance correlation with drilled records of drift deposits on the Antarctic Peninsula rise (Leg 178; e.g., Acton et al., 2002). However, the interpretations suggest equally high sedimentation rates for the Pleistocene, Pliocene, and upper Miocene.

Seven holes (U1532A–U1532G) were drilled in 3962 m water depth (Figure **F5**). The deepest hole (U1532G) was drilled to 794 m. Overall core recovery was 90%. Although sea ice was not a problem for the R/V *JOIDES Resolution* at this site, icebergs of various sizes, from large tabular icebergs to smaller fragments and growlers, frequently approached the ship and were the primary reason for the large number of holes. Holes U1532E and U1532F were nothing more than unsuccessful attempts to start coring at depth before being forced to avoid another approaching iceberg.

Lithostratigraphy

Deposits recovered at Site U1532 include silty clay with dispersed sand and gravel and variable biogenic content from five holes down to a recovered core depth of 787.4 m. Six lithofacies were identified based on visual characteristics of the sediments combined with information from smear slides and thin sections. Whole-core X-radiographs aided in observations of sedimentary structures, clast occurrence, and drilling disturbance. The dominant lithofacies assemblages are planar thinly laminated silty clay with episodic occurrences of massive and bioturbated silty clay typically <1.5 m thick. We observed dispersed sand grains, granules, and occasional pebbles throughout the assemblages, but they appear mainly concentrated within the massive and bioturbated facies. Minor lithofacies include foraminifer-rich and biosiliceous-rich mud to ooze.

We identified one lithostratigraphic unit with three subunits based on changes in facies assemblages: Subunits IA (0–92.6 m; Pleistocene–Pliocene), IB (92.6–400.6 m; Pliocene), and IC (401.0–787.4 m; Pliocene–Miocene). The sediments are mostly unconsolidated in the upper 150 m and become increasingly more consolidated below this depth. Intervals of carbonate-cemented laminae and very thin beds of coarse siltstone and sandstone are present deeper than 400 m.

Biostratigraphy

In the upper part of the section recovered at Site U1532 (i.e., Subunit IA; 0–92 m), sufficient microfossils for biostratigraphic age assignment were only present in the upper ~10 m, providing an age of middle Pleistocene to recent (0.0–0.6 Ma). Based on diatom and radiolarian biostratigraphy, ~92–156 m is assigned a mid- to late Pliocene age of 3.2–3.8 Ma and ~156–224 m is assigned an early Pliocene age of 3.8–4.4 Ma. The absence of microfossils or only trace occurrences of highly fragmented and recrystallized siliceous microfossils in samples deeper than ~224 m in Hole U1532G precluded shipboard biostratigraphic age determination at most levels. Exceptions include short intervals with poorly preserved but identifiable diatoms between ~224 and 332 m (early Pliocene; <4.7 Ma) and between ~332 and 510 m (early Pliocene to near the Miocene/Pliocene boundary; <5.5 Ma).

Some light green, biosiliceous-rich intervals coincide with higher concentrations of coarse sand and gravel, which are inferred to be IRD, and are generally bioturbated. Other intervals that were sampled based on their lower density than the laminated silty clay(stone) have a greenish color and show evidence of bioturbation but lack identifiable biosiliceous material, which we infer, at least in part, to reflect a diagenetic loss of diatoms and other siliceous microfossils. Organic microfossils occur throughout the Site U1532 sequence. A possibly in situ dinoflagellate cyst (dinocyst) assemblage of very low diversity and low abundance is present throughout the section but is most persistent deeper than 591.77 m. Calcareous microfossils including foraminifers, calcareous nannofossils, and ostracods generally occur in the absence of biosiliceous material in thin intervals in the Pleistocene section.

Paleomagnetism

The interpreted magnetic polarity at Site U1532 was correlated with the Geomagnetic Polarity Timescale (GPTS) of Gradstein et al. (2012). The resulting key paleomagnetic data were then integrated with biostratigraphic data to produce an age model.

For Hole U1532A, we obtained reliable shipboard magnetostratigraphy that consists of four normal and four reversed polarity intervals. The Brunhes–Matuyama polarity transition (0.781 Ma), the termination and beginning of the Olduvai Subchron (1.778 and 1.945 Ma, respectively), the Matuyama–Gauss polarity transition (2.581 Ma), the termination and beginning of the Kaena Subchron (C2An.1r; 3.032 and 3.116 Ma, respectively), and the termination and beginning of the Mammoth Subchron (C2An.2r; 3.207 and 3.330 Ma, respectively) were identified. Paleomagnetic measurements for Hole U1532B identified the beginning of the Mammoth Subchron (C2An.2r; 3.330 Ma) and the Gauss–Gilbert polarity transition (3.596 Ma). Paleomagnetic measurements for Hole U1532C identified the termination of the Nunivak Subchron (C3n.2n; 4.493 Ma) but no clear Cochiti Subchron (C3n.1n; 4.187–4.300 Ma). Natural remanent magnetization (NRM) measurements for Hole U1532G identified the beginning of the Nunivak Subchron (C3n.2n; 4.631 Ma), the termination and beginning of the Sidufjall

Subchron (C3n.3n; 4.799 and 4.896 Ma, respectively), and the termination and beginning of the Thvera Subchron (C3n.4n; 4.997 and 5.235 Ma, respectively). Reversed magnetic polarity continues downhole to the bottom of Hole U1532G. The beginning of Chron C3r (6.033 Ma) was not observed. Therefore, the oldest sediments recovered at Site U1532 are presumably of late Miocene age.

Geochemistry

At Site U1532, 65 interstitial water samples were collected and measured for salinity, alkalinity, pH, major ions (Na, K, Ca, Cl, and SO_4), nutrients (NH_4 and PO_4), silica ($H_4Si(OH)_4$), and trace elements (Sr, Li, Fe, Mn, B, and Ba). Drilling fluid contamination was detected in a few interstitial water samples taken from XCB cores. Higher abundances of perfluorocarbon tracer in these samples are in line with this observation. The SO_4 downhole profile shows a sharp linear decrease from ~28 mM near the surface to ~2.3 mM at ~664 m; however, SO_4 concentration did not reach zero at this site, indicating a low SO_4 reduction rate. The Ca and Sr profiles show an overall increase, whereas the K and Mg profiles display the reverse trend. Silica concentration is relatively high from 8.5 to 238 m, coinciding with intervals where a higher abundance of diatoms was observed. Diagenesis of diatoms through reaction with the interstitial water likely results in higher silica concentration.

Calcium carbonate ($CaCO_3$) content is low in the sediments of Lithostratigraphic Subunit IA; discrete maxima in $CaCO_3$ observed in the upper section of Subunit IA are linked to layers rich in calcareous foraminifer tests. Subunit IB is characterized by a general increase in $CaCO_3$ downhole. Total organic carbon (TOC) content is generally low at Site U1532 but displays a stepwise increase from Subunit IA to Subunit IC. Total nitrogen content is low throughout all subunits. Total sulfur (TS) content decreases throughout Subunit IA and generally remains low throughout Subunit IB. TS displays a downhole increase in the uppermost section of Subunit IC (to ~533 m). Deeper than ~533 m, TS declines again and then shifts to low values deeper than ~670 m. This shift in TS content is associated with a near depletion of interstitial water sulfate concentrations, which may limit sulfate reduction.

Headspace gas samples to monitor for the presence and abundance of C_1–C_3 hydrocarbons indicate that methane occurs in only very low concentrations throughout the upper ~650 m. At ~667 m, methane concentration increases rapidly, exceeding 5000 ppmv deeper than ~713 m and reaching a maximum of 9517 ppmv at ~771 m. The increase of methane at ~667 m coincides with a pronounced minimum in sulfate, suggesting that methane may be biogenic at Site U1532.

Physical properties

Collected physical property data include magnetic susceptibility, natural gamma radiation (NGR), gamma ray attenuation (GRA) bulk density, discrete moisture and density (MAD), *P*-wave velocity, thermal conductivity, in situ formation temperature (advanced piston corer temperature tool [APCT-3]), and spectral color reflectance. Whole-round magnetic susceptibility trends follow those observed in GRA bulk density and NGR, likely indicating changes in terrigenous sediment content. Magnetic susceptibility data were used as a primary tool for correlating cores from adjacent holes. In the upper 65 m, bulk density increases downhole from ~1.5 to ~1.8 g/cm^3, followed by a more gradual increase to ~2.2 g/cm^3 in the deeper section, reflecting increasing compaction. Intervals of significantly lower density correspond to greenish gray intervals in Lithostratigraphic Subunits IB and IC. Sediment porosity decreases downhole from 77% at the seafloor to 60% at 30 m and decreases further with depth to 35% at the bottom of Hole U1532G, reflecting the downward compaction trend of marine sediments. *P*-wave velocity increases with depth from ~1460 m/s at the seafloor to ~2000 m/s at the base of Hole U1532G. No major changes in *P*-wave velocity were observed across the lithostratigraphic subunit boundaries. Overall, thermal conductivity increases with depth from ~1 W/(m·K) at the seafloor to ~1.8 W/(m·K) at ~390 m, corresponding to a downhole increase in dry bulk density and decrease in porosity because of compaction. Formation temperature measurements from 34.0 to 150.0 m in Hole U1532A were used to estimate a geothermal gradient of ~54°C/km.

Site U1533

Background

Site U1533 (proposed Site ASRE-09A) is located 62 km west-southwest of Site U1532 on the westernmost lower flank of Resolution Drift, the same sediment drift as Site U1532, on the continental rise of the Amundsen Sea (Figures **F1**, **F6**). This lower flank is bound by a north-south–oriented deep-sea channel west of Site U1533 (Uenzelmann-Neben and Gohl, 2012). The channel is likely the path of sediment transported downslope from the shelf by turbidity currents and sediment gravity flows and, as such, is likely the major source of terrigenous sediment to the drill site (e.g., Dowdeswell et al., 2006). Bottom currents transported clay- and silt-sized particles before they deposited them to form a drift (e.g., Nitsche et al., 2000). A robust horizon correlation from Site U1532 was performed along three connected seismic lines, indicating that sedimentary sequences of the same age are more condensed at Site U1533.

Four holes (U1533A–U1533D) were drilled at Site U1533 in water depths between 4179 and 4184 m (Figure **F7**). The deepest penetration (Hole U1533B) reached 383 m with an overall core recovery of 70%. As at Site U1532, frequent approaches of icebergs of various sizes were the primary reason for the large number of holes.

Lithostratigraphy

Sediments recovered at Site U1533 consist mainly of silty clay with varying biogenic content and amounts of bioturbation as well as rare occurrences of diamict and conglomerate. Thin sand and silt beds and laminae occur throughout, and intervals of carbonate cementation and volcaniclastic material were also observed. The recovered sediments are categorized into seven lithofacies based on visual characteristics and lithologic information supported by smear slide observations. The drilled sequence is divided into Lithostratigraphic Subunits IA and IB based on changes in facies assemblages. Whole-core X-radiographs were used to aid in the identification of sedimentary structures, clast occurrence, and drilling disturbance. Site U1533 is dominated by deposition of fine-grained sediments interpreted to be initially supplied by sediment gravity flows from the continental shelf and subsequently reworked by contour currents. Silt and sand beds are interpreted to have been deposited by overspill of turbidity currents from the submarine channel. Additionally, a significant amount of biosiliceous material in the sediments is supplied from the overlying surface waters.

The association of facies in Lithostratigraphic Subunit IA predominantly reflects the interplay of downslope and contouritic sediment supply that also includes input of more pelagic sediment during phases of seasonally open marine conditions. The amount of biogenic material is generally high throughout Subunit IA, suggesting relatively sustained periods of high marine productivity. Deposits related to downslope transport are present throughout the sedimentary record at Site U1533. In Subunits IA and IB, coarse-grained beds probably indicate that overspill deposition originated from downslope transport through the adjacent deep-sea channel. Subunit IB has generally higher amounts of visible clasts and pebbles than Subunit IA. Dispersed granules and pebbles, clast nests, and discontinuous bands of coarse sand and granules in Subunits IA and IB are inferred to indicate persistent but likely low-intensity ice rafting, and there is a higher abundance of this IRD within diatom ooze intervals.

Biostratigraphy

In contrast with Site U1532, which contains significant intervals that are barren of microfossils, the majority of Site U1533 samples from the mudline to the lowermost sediments contain microfossils. Preservation and abundance of microfossils are highly variable, including some barren intervals noted in the uppermost Pliocene–lowermost Pleistocene and lower Pliocene sections. A similar general pattern of alternating gray-beige to brownish sediments (Lithostratigraphic Subunit IA) and gray-beige to greenish sediments (Subunit IB) at Site U1532 was commonly observed at Site U1533 and consisted of gray, laminated, microfossil-poor, mostly terrigenous mudstones punctuated by thinner brownish to greenish bioturbated, variably biosilica-bearing intervals, some with sand to pebble-sized material interpreted to be IRD. However, the brownish and greenish bioturbated units have a higher overall concentration of biosiliceous material than at Site U1532.

The upper ~40 m of Site U1533 spans the Pleistocene and contains variable concentrations of diatoms, radiolarians, and foraminifers; rare marine and reworked terrestrial palynomorphs; and very rare calcareous nannofossils. Diatoms and radiolarians are present in most samples examined from this interval. Foraminifers are present only in a few intervals in the upper ~10 m of the sequence.

Pleistocene to upper Miocene sediments recovered from Hole U1533B are dated primarily by diatoms and radiolarians. Both are documented with variable abundance from the top to the bottom of Hole U1533B. Samples from the lowermost cores generally contain common to abundant diatoms, although the assemblages are highly fragmented. Diatoms and radiolarians provide a latest Miocene age (6.2–6.7 Ma) for the lowermost sediments recovered from Hole U1533B; combined with magnetostratigraphic constraints, the deepest sediments recovered in Hole U1533B are ~6.4–6.75 Ma. Foraminifers and calcareous nannofossils were not observed in the Pliocene sediments in Hole U1533B, whereas rare to common marine and reworked terrestrial palynomorphs are present throughout the hole.

Paleomagnetism

For Hole U1533A, demagnetization of NRM at 20 mT identifies the Brunhes–Matuyama transition (0.781 Ma), the termination and beginning of the Jaramillo Subchron (C1r.1n; 0.988 and 1.072 Ma, respectively), and the termination and beginning of the Cobb Mountain Subchron (C1r.2n; 1.173 and 1.185 Ma, respectively).

The magnetostratigraphy for Hole U1533B is more complex than for Hole U1533A because of reduced core recovery and drilling disturbance of some intervals. The shipboard interpretation identifies the beginning of the Olduvai Subchron (C2n; 1.945 Ma), the termination and beginning of Subchron C2An.1n (2.581 and 3.032 Ma, respectively), the termination and beginning of Subchron C2An.3n (3.330 and 3.596 Ma, respectively), the termination and beginning of the Cochiti Subchron (C3n.1n; 4.187 and 4.300 Ma, respectively), and the termination and beginning of the Nunivak Subchron (C3n.2n; 4.493 and 4.631 Ma, respectively). Subchron C2An.2n (3.116–3.207 Ma) might be present in a very condensed form in Core 379-U1533B-5H at ~58 m. Further downhole, paleomagnetic measurements reveal the termination and beginning of the Sidufjall Subchron (C3n.3n; 4.799 and 4.896 Ma, respectively) and the termination and beginning of the Thvera Subchron (C3n.4n; 4.997 and 5.235 Ma, respectively). Below an interval without core recovery, the oldest cores, 39R and 43R, are of mainly normal polarity, suggesting a bottom age for Hole U1533B between the termination of Subchron C3An.1n (6.033 Ma) and the beginning of Subchron C3An.2n (6.733 Ma). Oscillating normal and reversed polarity at the bottom of Hole U1533B provides no clear evidence that Subchron C3Ar was recovered.

For Hole U1533C, no magnetic polarity reversal was recorded, suggesting that the recovered sediments are younger than the Brunhes–Matuyma transition (0.781 Ma).

For Hole U1533D, paleomagnetic measurements identified the Brunhes–Matuyama transition (0.781 Ma), the termination and beginning of the Jaramillo Subchron (C1r.1n; 0.988 and 1.072 Ma, respectively), the termination and beginning of the Cobb Mountain Subchron (C1r.2n; 1.173 and 1.186 Ma, respectively), and the termination and beginning of the Olduvai Subchron (C2n; 1.778 and 1.945 Ma, respectively).

Chronostratigraphy

By combining biostratigraphy and magnetostratigraphy, the interval shallower than ~37 m is assigned a Pleistocene age, ~37–265 m is assigned a Pliocene age, and ~265–383 m (base of recovery at Site U1533) is assigned a latest Miocene age. The combined data indicate a 6.4–6.75 Ma age for the base of Hole U1533B at 381.23 m.

Geochemistry

Interstitial water salinity at Site U1533 is constant at 35 from the seafloor to ~235 m and is slightly lower (33 to ~34) from 255 to 375 m. Chloride (Cl) concentration ranges between 557 and 596 mM, with the latter concentration being slightly higher than the average concentration in modern seawater (~559 mM). The elevated Cl could be due to hydration reactions during clay formation. Sodium (Na) concentration ranges between 440 and 483 mM throughout the section. Deeper than ~17 m, sulfate (SO_4) decreases continuously with depth and reaches its minimum (~1.6 mM) at 375 m. Interstitial water alkalinity increases linearly with depth from 1.5 m to a maximum (~10.5 mM) at ~185 m, which is the opposite trend to that of SO_4. Deeper than ~185 m, alkalinity slightly decreases with depth to 255 m.

Strontium (Sr) concentration increases overall from 85 µM at 1.5 m to 196 µM at 255 m, reaching maximum values ~2 times higher than that of the modern seawater value (87 µM). The higher Sr concentration indicates either higher fluid-rock reaction with volcaniclastic material or dissolution of carbonates.

Methane concentration is ~4 ppmv, which is close to the instrumental background signal, in Hole U1533A and most of Hole U1533B. At 325.60 m, methane concentration abruptly increases downhole to a peak of 6373 ppmv at 375.02 m. No hydrocarbons other than methane were detected at Site U1533. Increased methane was found only at the base of Lithostratigraphic Subunit IB, where the lowest SO_4 was observed. Together with the absence of higher hydrocarbons, this suggests a biological source of methane at Site U1533.

Total carbon content varies between 0.02 and 0.5 wt% and increases with depth. $CaCO_3$ is low at Site U1533 and ranges between 0.02 and 2.54 wt%. TOC content varies between 0.01 and 0.41 wt% and is similar in terms of trends and abundances to the TC record, indicating that organic carbon constitutes most of the total carbon pool.

Samples for contamination testing were collected from the exterior and center of freshly exposed core sections or whole-round samples. Perfluorocarbon tracers were present in variable concentrations in samples taken from most APC core exteriors because of the direct exposure of the core surface to circulating drilling fluids. However, tracer concentrations are approximately four orders of magnitude lower in these samples than the target concentrations of tracers in the drilling fluid. Tracers were below detection in the interior of most APC and HLAPC cores. The absence of tracers in the central parts of most APC/HLAPC cores and their generally low presence in core exteriors suggest low overall contamination. XCB cores generally show low contamination in both the interior and exterior samples, but in contrast to APC/HLAPC cores, contamination was consistently present in the center of the cores. The sampled RCB cores generally showed higher levels of tracer contamination than APC/HLAPC and XCB cores.

Physical properties

Measured whole-round magnetic susceptibility ranges between 4.7×10^{-5} and 804.6×10^{-5} SI. Average magnetic susceptibility values increase downhole from ~50×10^{-5} to ~100×10^{-5} SI at ~55 m, which corresponds to the Lithostratigraphic Subunit IA/IB boundary. Within this general downhole increase, the upper ~15 m of Holes U1533A, U1533C, and U1533D exhibit a "saw-tooth" pattern of magnetic susceptibility cyclicity, wherein a sharp increase in overall magnetic susceptibility is followed by a more gradual decline. Magnetic susceptibility data were used as a primary tool for correlating cores from adjacent holes to create a shipboard splice for the uppermost ~44 m of the site. Measured NGR ranges between 13.5 and 235.1 counts/s with an overall average of 56.1 counts/s. Average NGR values increase downhole from ~20 counts/s at the mudline to ~75 counts/s at ~55 m, which corresponds to the Subunit IA/IB boundary. Deeper than ~55 m, NGR varies cyclically between ~20 and 75 counts/s. NGR values follow trends observed in magnetic susceptibility and GRA bulk density values except for the saw-tooth variability observed in the upper parts of the holes, which likely indicates changes in the ratio between biogenic and terrigenous sediment content. The GRA bulk density record shows a sharp downhole increase from ~1.3 to ~1.8 g/cm^3 in the uppermost ~55 m that corresponds to Subunit IA. Below this depth, GRA density exhibits several stepwise changes. The overall increase in GRA bulk density with depth at this site reflects the increasing compaction of sediment with depth. Smaller scale variability indicates changes in sediment lithology and correlates well with NGR and magnetic susceptibility variability. MAD bulk density increases sharply downhole from ~1.3 g/cm^3 at the seafloor to ~1.7 g/cm^3 at ~50 m, corresponding to a sharp decrease in porosity and void ratio. From ~50 m to the bottom of Hole U1533B at ~383 m, bulk density increases more gradually.

P-wave logger (PWL) velocity increases with depth, ranging from ~1480 m/s at the seafloor to ~1620 m/s at ~205 m. *P*-wave caliper (PWC) measurements track well with the PWL measurements for the upper ~205 m, showing a gradual increase with depth. PWC velocity continues to increase as consolidation increases with depth to an average velocity of ~1780 m/s at ~380 m.

Thermal conductivity increases with depth from ~0.7 W/(m·K) at the seafloor to ~1.4 W/(m·K) at ~375 m and corresponds to a downhole increase in dry bulk density and decrease in porosity from compaction.

Preliminary scientific assessment

Operational considerations related to the science objectives

Expedition 379 accomplished drilling and coring at two very successful sites on the continental rise of the Amundsen Sea. Drilling at Site U1532, on a large sediment drift, penetrated to 794 m (90% recovery), making this site the deepest drilled in West Antarctica with a ship-based rig and resulting in the longest drill core recovered in all of Antarctica drilled with a ship-based rig. We collected almost continuous core from the Pleistocene through the Pliocene and into the late Miocene. At Site U1533, we drilled to 383 m (70% recovery) into the more condensed sequence at the lower flank of the same sediment drift. The cores from both sites contain unique records with which to study the cyclicity of ice sheet advance and retreat processes as well as bottom-water circulation and water mass changes. In particular, Site U1532 revealed a sequence of Pliocene lithofacies with an excellent paleomagnetic record for high-resolution climate change studies of the previously sparsely sampled Pacific margin of West Antarctica.

Despite the drilling success at both sites, the overall expedition experienced three difficulties that affected many of the scientific objectives of all five hypotheses of Proposal 839 and the *Scientific Prospectus*:

1. The extensive sea ice on the continental shelf prevented us from drilling any of the primary proposed sites located on the shelf. The two sites that we did successfully drill were added to the project in early 2018 after the record-setting sea ice that austral summer covered all approved primary and alternate sites from the proposal, forcing the creation of additional alternate plans. The sea ice remaining from 2018 became multiyear ice in 2019, limiting the breakout that could happen in a single season. During Expedition 379, sea ice was never at a level low enough for *JOIDES Resolution* to enter the shelf, even when sea ice became less concentrated between the continental rise and the open-water polynya where many of the shelf sites are located.
2. On the continental rise, we faced a steady stream of icebergs of various sizes that approached the ship and frequently forced us to pause drilling or leave the hole entirely. The overall downtime caused by approaching icebergs was 50% of our time spent on site (Table **T1**). This large iceberg abundance in the Amundsen Sea during the austral summer was possibly unprecedented and may have been caused by major calving events of the ice shelves during the last 2–3 y.
3. Because of an unfortunate injury to a member of the ship's crew, we had to cut the expedition short by one week. Before the accident, which led to a medical evacuation, we intended to complete Site U1533 by coring all of the Miocene and possibly into the Oligocene, complete downhole logging for the first time during the expedition, and collect APC cores at proposed Primary Site ASRE-05B near the foot of the continental slope, which had become accessible in the days before. Although all three of these goals likely would not have been possible in the last 7 days of the cruise, it is likely at least two of them would have been achieved.

Because of these three unexpected and extreme circumstances, we were unable to achieve many important objectives, including obtaining ice-proximal shelf records and collecting cores from the Mid-Miocene Climatic Optimum, the Oligocene/Miocene boundary, and the Eocene–Oligocene transition. Drilling sites are needed to obtain ice-proximal records from these transitions for a full understanding of the proximal glacial history in this region, which is one of the key components of IODP's transect approach to understanding high-latitude climate history. The Expedition 379 sites were designed to obtain records of past warm deep-water incursions onto the shelf that are the cause of present melting. Models suggest that the current incursion of warm deep-water to the base of the ice is an unsustainable situation, but we do not yet have records showing whether warm water has encroached onto the shelf in the past and, if so, how the ice responded. The study of such records from the shelf is one of the central scientific objectives of the proposal for Expedition 379.

Preliminary assessment of scientific objectives

The scientific objectives for this expedition were built on five hypotheses about the dynamics of the WAIS and related paleoenvironmental and paleoclimatic conditions. Based on a preliminary analysis of the core material and data collected during the expedition, we assess each of the five hypotheses below.

From the outset, Expedition 379 included a wide range of primary and alternate sites to allow for drilling in a range of sea ice conditions. All five objectives were addressed at most sites, both primary and alternate. However, the third tier of drill targets on the continental rise, proposed in case of extreme sea ice cover, could only be used to address the first three hypotheses directly, and unfortunately these third-tier sites were the only sites achieved during Expedition 379. Nonetheless, high-quality core recovery combined with slight modifications to our research approach allows each hypothesis to be addressed to some degree.

Sites U1532 and U1533 are located on a sediment drift deposit, the Resolution Drift, on the continental rise north of the Amundsen Sea Embayment shelf edge (Figure **F1**). Coring at both sites recovered relatively undisturbed sequences from the late Miocene to Quaternary.

Coring at Site U1532 recovered silty clay with dispersed sand and gravel and variable biogenic content in five holes to a core depth of 787 m (Figures **F4**, **F8**). Linear sedimentation rate calculated between magnetostratigraphic age control points shows a significant downcore increase in sedimentation rate that averages ~2 cm/ky in the Pleistocene, ~18 cm/ky in the middle Pliocene, and ~41 cm/ky in the latest Miocene to early Pliocene section. The highest sedimentation rate documented, ~61 cm/ky, is between 4.49 and 4.63 Ma. The lowest sedimentation rate in the Pliocene section (~10 cm/ky) is calculated between 4.63 and 4.80 Ma and may indicate a transient decrease in sediment flux to the site or possibly the presence of a short hiatus in this interval.

Sediments recovered at Site U1533 consist mainly of silty clay with varying biogenic content and amount of bioturbation and rare occurrences of diamict and conglomerate intervals. Four holes were drilled at this site, reaching a total core depth of 382.6 m (Figures **F6**, **F9**). Similar trends in sedimentation rates are documented at Sites U1532 and U1533, but sedimentation rates are 2–3 times lower at Site U1533. Linear sedimentation rate shows an overall downcore increase in accumulation rate, which averages ~1.4 cm/ky in the Pleistocene, ~5.4 cm/ky between ~4.5 and 2.6 Ma in the Pliocene, and ~15.5 cm/ky between ~5.2 and 4.5 Ma in the earliest Pliocene. The highest sedimentation rate (~21–22 cm/ky) at Site U1533 is in the early Pliocene between 4.493 and 4.631 Ma and between 4.997 and 5.235 Ma. The lowest sedimentation rate in the Pliocene section of Site U1533 (~3 cm/ky) is between 4.631 and 4.799 Ma. A similar decrease in sedimentation rate is thus inferred for the same time interval at Sites U1532 and U1533 and Leg 178 Site 1095 on the Antarctic Peninsula (Acton et al., 2002), which may indicate a regional decrease in terrigenous sediment flux between 4.63 and 4.80 Ma.

Hypothesis H1: the WAIS responded to atmospheric and oceanic warming by a major retreat from the shelf or by even partial to full collapse.

A primary goal of Expedition 379 is to reconstruct the glacial history of West Antarctica from the Paleogene to recent times with a focus on the dynamic behavior of the WAIS during the Neogene and Quaternary, especially possible partial or even full WAIS collapses. Particular emphasis is placed on studying the response of the WAIS at times when the pCO_2 in Earth's atmosphere exceeded 400 ppm and atmospheric and oceanic temperatures were higher than at present.

Recovery of core on the continental rise at Sites U1532 and U1533 cannot give a direct answer regarding the configuration of glacial ice on the shelf or retreat of the ice sheet across the shelf. However, the sediments contained in the cores offer a range of clues about past ice sheet extent and retreat. At both sites, coarse-grained sediments interpreted to be IRD were identified throughout all recovered time periods. Cyclicity is a dominant feature of the cores and is interpreted to represent relatively warmer periods variably characterized by higher microfossil abundance and higher counts of ice-rafted debris alternating with colder periods characterized by dominantly gray laminated terrigenous muds. A revised age model will be completed after the expedition, and tuning of Expedition 379 data sets to precise time periods will follow. However, an initial comparison of these cycles with published late Pleistocene records from the region (e.g., Hillenbrand et al., 2009) suggests that the units interpreted as records of warmer time intervals in the cores are tied to interglacial periods and the units interpreted as deposits of colder periods are tied to glacial periods. Postexpedition work to determine IRD accumulation rates over time will allow identification of pulses of glacial sediment input that may be representative of major calving events.

More specific evidence of major collapse will come from studying the provenance of the IRD at the drill sites. IRD pulses often represent major calving events, although the signal can be ambiguous because it may simply be a local increase in accumulation or, barring detailed age constraints, a signal of decreased flux of fine-grained material. Therefore, layers rich in IRD will be targets for more detailed studies aimed at identifying the provenance of the IRD. Coarse grains will be identified by visual description and geochemical analyses that will also be applied to fine-grained detritus, including Sr-Nd signatures, to determine the source of glacigenic sediment deposited on the Resolution Drift. A change in provenance over time at the site will be an indication of varying positions of the grounding line. Specific isotopic signatures, including Pb isotopes, will be used to identify patterns of bedrock weathering that may indicate specific source rocks were exposed subaerially. Additionally, different clay mineral signatures with geochemical analyses (including Sr-Nd) in the fine-grained fraction may be identified as having come from specific regions onshore, allowing further identification of the source of sediment shed to the region and thus indicating how far the ice may have retreated.

These combined signals will allow reconstruction of the ice sheet since the late Miocene based on the amount and source of sediment shed to the region. Results from ANDRILL Core AND-1B suggest repeated WAIS collapses during warm early middle Pliocene and Pleistocene interglacials (e.g., during MIS 31) (Naish et al., 2009; Pollard and DeConto, 2009; McKay et al., 2012; Villa et al., 2012). The hypothesis of WAIS collapse needs confirmation with a less ambiguous record from an outlet drainage basin exclusively affected by the WAIS. The cores recovered during Expedition 379 cannot give such unambiguous information; however, the records of glacigenic sediment delivery to the sites will give an integrated signal that will record major changes in ice sheet extent.

Hypothesis H2: ice-proximal records of ice sheet dynamics in the Amundsen Sea correlate with global records of ice-volume changes and proxy records for atmospheric and ocean temperatures.

A goal of Expedition 379 is to correlate the WAIS-proximal records of ice sheet dynamics in the Amundsen Sea with global records of ice volume changes and proxy records for air and seawater temperatures. As described above, the initial interpretation of cores from Sites U1532 and U1533 shows repeated alternations between different facies interpreted to represent glacial–interglacial cycles. Comparison with dated gravity and piston cores nearby (e.g., Hillenbrand et al., 2002, 2009) suggest that the cycles identified in cores from both sites are correlative with global oxygen-isotope records. The pattern holds at least as far back as MIS 35, and thus several “superinterglacials” have been recovered. Ongoing work will focus on tuning the age model, particularly for Pliocene warm intervals that are not yet well constrained, to confirm these initial interpretations and allow more detailed analysis, including deconvolving the glacial–interglacial signals from what may be independent changes in ocean currents bringing sediment to the drill sites.

Work on proxies will be conducted to determine paleoceanographic characteristics, including temperature, salinity, current speed, and water mass origins. These data, which are independent of the specific age model, will allow the record of ice sheet fluctuations to be tied to local temperature and current information as well as to the global records of ice volume.

Hypothesis H3: the stability of marine-based WAIS margins is and has been controlled by warm deep-water incursions onto the shelf.

Today, the dramatic Amundsen Sea sector ice loss is attributed to incursions of warm CDW reaching the base of the ice shelves fringing the WAIS (Joughin et al., 2014). Such incursions have been identified in the Holocene (Hillenbrand et al., 2017; Minzoni et al., 2017) and recent sediments (Smith et al., 2017), but it is unclear how often such incursions have happened farther in the past or how the ice may have responded. Therefore, another goal of Expedition 379 is to study the relationship between incursions of CDW onto the continental shelf of the Amundsen Sea Embayment and the stability of marine-based ice sheet margins under such warm-water conditions. Postexpedition work will try to fingerprint water masses flowing across the drill site, and multiple proxies will estimate water temperature, including both lipid paleothermometers and foraminifer stable isotopes. However, most of these analyses will yield details of either surface water or bottom-water masses, not the middle-depth signature of CDW, mainly because of the lack of proxies that can yield clear information for that middle depth. Nonetheless, estimates of broad-scale temperature changes will be tied to IRD and other records of ice sheet change, allowing correlation between temperature at the drill sites and ice behavior.

Hypothesis H4: major WAIS advances onto the middle and outer shelf have occurred since the middle Miocene.

The aim during Expedition 379 was to obtain records from various sites on the shelf of the Amundsen Sea Embayment from unconformities within strata that document frequent advance and retreat of grounded ice from the late Miocene until the Pliocene/Pleistocene. Seismic data reveal progradational and aggradational deposition on the outer shelf and slope probably since the mid-Miocene (e.g., Nitsche et al., 1997, 2000; Hochmuth and Gohl, 2013; Gohl et al., 2013b). The seismic stratigraphic age model of the shelf sequences by Gohl et al. (2013b) is only constrained by far-distance correlation of seismic reflection characteristics and pattern with those observed and age-dated from the Ross Sea shelf (e.g., De Santis et al., 1999) because of the lack of deep drill sites on the Amundsen Sea shelf. The fact that we were unable to access the open-water polynya on the middle shelf with *JOIDES Resolution* during Expedition 379 because of sea ice on the outer shelf prevented us from obtaining such direct shelf records.

The drill cores from both rise sites, however, recovered sediments of terrigenous origin intercalated or mixed with pelagic or hemipelagic deposits. In particular, Site U1533, which is located near a deep-sea channel running from the lower continental slope to the abyssal plain, contains graded beds as well as clasts transported downslope from the shelf by turbidity currents or other gravitational transport processes.

The association of lithologic facies in both sites predominantly reflects the interplay of downslope and contouritic sediment supply with more pelagic sediment input during phases of seasonal-open marine conditions, which is consistent with a greater amount of biogenic material and suggests relatively sustained periods of relatively high marine productivity. Recovered dispersed granules and pebbles, clasts, and discontinuous bands of coarse sand and granules in the cores are inferred to indicate persistent but likely low-intensity ice rafting that may have increased periodically during warmer periods. Because these observations can be made throughout the Pleistocene and Pliocene and into the late Miocene, we can infer from drilling that grounded ice frequently covered most of the Amundsen Sea shelf since at least the late Miocene.

Despite the lack of drill cores from the shelf, our records from the continental rise reveal the timing of glacial advances onto the shelf and thus the existence of a continent-wide ice sheet in West Antarctica for prolonged periods since at least the late Miocene. Hypotheses of earlier phases of WAIS expansion in the Amundsen Sea sector remain untested by drill records.

Hypothesis H5: the first WAIS advance onto the inner Amundsen Sea continental shelf occurred during the Oligocene and was related to the uplift of Marie Byrd Land.

The relationship between the onset of major West Antarctic glaciation and the continental paleotopography necessary for growing a substantial ice sheet has so far only been addressed by numerical modeling (DeConto and Pollard, 2003; Wilson et al., 2013). Such modeling indicates an elevated Marie Byrd Land might be required for a large ice sheet to form in the Amundsen Sea/Marie Byrd Land sector. Seismological models show that a low-velocity, presumably hotter than normal mantle exists beneath Marie Byrd Land today (e.g., Lloyd et al., 2015). The objective of Expedition 379 is to reveal evidence from drill records that will allow a reconstruction of the timing and rates of an uplift that has been inferred by studies of the Marie Byrd Land dome exhumation and erosion history (e.g., Rocchi et al., 2006; Wilson and Luyendyk, 2009; Wilson et al., 2012, 2013; Spiegel et al., 2016). The latest thermochronological study suggests an uplift not earlier than early Miocene (Spiegel et al., 2016).

Although we were unable to drill cores for detailed provenance and thermochronological analyses of samples from the shelf, cores from both rise sites contain abundant coarse-fraction sediments and clasts of plutonic origin transported either by downslope processes or by ice rafting. The common lithic types are polycrystalline quartz and K-feldspar granite. Biotite-bearing leucogranite and diorite are also present. If detailed provenance studies confirm our preliminary assessment that the origin of these samples is plutonic bedrock of Marie Byrd Land, their thermochronological record will potentially reveal timing and rates of denudation and erosion linked to crustal uplift.

The chronostratigraphy of both drill sites enables the generation of a seismic sequence stratigraphy not only for the Amundsen Sea rise but also for the western Amundsen Sea along the Marie Byrd Land margin through a connecting network of seismic lines. A detailed analysis of correlated seismic unit boundaries and unconformities will allow reconstruction of the Marie Byrd Land dome uplift at least back to the earliest age-dated horizons of the late Miocene and, with an appropriate seismic stratigraphic age model using estimates on earlier sedimentation rates, possibly even back to the Oligocene or earlier.

In addressing the objectives of this hypothesis, the thermochronological analyses and seismic sequence stratigraphy will make use of the drilled core samples and the core data from independent methods to test the hypothesis of the Marie Byrd Land uplift and its role in early ice sheet evolution.

Operations

We conducted operations in 7 holes at Site U1532 (Proposed Site ASRE-08A) and 4 holes at Site U1533 (Proposed Site ASRE-09A) (Table **T1**). At Site U1532, coring penetrated to 794.0 m with an overall recovery of 90%. At Site U1533, we cored to a total depth of 382.6 m with

- Multiple holes recovering a complete stratigraphic section in the uppermost 50 m,
- Excellent recovery with APC/HLAPC coring downhole to 205.8 m,
- Moderate recovery (63%) with XCB coring from 205.8 to 283.9 m, and
- Low recovery (15%) from 283.9 to 382.6 m.

We spent a total of 23.7 days at Site U1532 and 11.68 days at Site U1533. Drifting icebergs caused multiple interruptions that resulted in nearly half of this time at both sites (11.46 and 5.22 days, respectively) being spent waiting for ice to clear the area or performing operations not originally planned (pipe trips, reentries, abandoned holes, or repeated drilled intervals). The frequency of interruptions caused by drifting icebergs and significant variations in their speed and direction proved problematic. Ultimately, deployment of a free-fall reentry system shortly after starting to drill into the seafloor was required for us to penetrate deeply at each site (794.0 m in Hole U1532G and 382.6 m in Hole U1533B).

We had to stop drilling operations 6.2 days earlier than originally planned (at 1448 h on 7 March 2019) to return to Chilean waters to evacuate an injured crew member.

Unless otherwise noted, all depths are calculated as core depth below seafloor, Method A (CSF-A), and are reported as "m." All times in this report are in ship local time (UTC – 3 h). In this section, we also document the start of the expedition in Punta Arenas, Chile, the transits to Sites U1532 and U1533, drilling operations at the sites, and the transit back to Punta Arenas.

Punta Arenas port call and transit to Site U1532

The Amundsen Sea Expedition was planned to start on 18 January 2019. However, the ship arrived a few days early (15 January) after the long transit from Hong Kong. This time was used to load special Antarctic fuel on 15–16 January at the Cabo Negro Oil Terminal. The ship departed Cabo Negro at 1206 h on 16 January and was at anchorage off Punta Arenas, Chile, at 1438 h on 16 January. The ship left anchorage at 0548 h on 17 January, and after a very short transit arrived at the Prat Terminal 2, Punta Arenas, at 0730 h. The rest of the day was spent loading and installing a critical piece of drilling hardware (repaired J-connector) and a few other available supplies. Expedition 379 Amundsen Sea officially started at 0800 h on 18 January with the Co-Chief Scientists and staff of the *JOIDES Resolution* Science Operator (JRSO) boarding the ship. The JRSO staff conducted their crossover with the departing staff who left later in the afternoon. Other port call activities included a Port State Inspection and loading of 60 tons of drilling mud, a flat of drilling equipment, food and other catering supplies, and various IODP-JRSO and ship stores. The JRSO technical staff started with preparations to assemble and install the new X-ray system for acquiring images of core sections.

The Expedition 379 scientists boarded the ship on the morning of 19 January. After getting settled in their rooms, the scientists were introduced to life on board *JOIDES Resolution*, general laboratory safety, and information technology resources/services. Other port call activities included loading the final drilling hardware, securing all items for departure, and continued assembly and testing of an alternate satellite communication system because our normal system was not expected to work effectively in our area of operations.

On 20 January, the science party met to discuss the primary science objectives of the Amundsen Sea expedition and participated in the Captain's introduction and safety meeting. The Co-Chief Scientists, Operations Superintendent, Ice Observers, JRSO Assistant Director, JRSO Manager of Development, IT, and Databases, and Expedition Project Manager met to converge on shipboard procedures for ice and weather data to be used for science operational planning. We also loaded fresh and frozen food and secured equipment for departure. The JRSO technical staff continued with the final installation and testing of the new X-ray system.

On January 21, we continued securing equipment for departure and waited for the arrival of additional backup satellite communications systems required to maintain essential communications, a backup wireline logging tool (Versatile Seismic Imager [VSI]), and heaters for the life raft release system required under the polar code for us to sail. Also, the Captain was evaluating the weather to determine the optimum timing and route for departing Punta Arenas.

The backup wireline logging tool (VSI) and the essential backup satellite communications systems were received on 22 January. Installation of the backup communications systems began immediately while waiting for the heaters for the life raft release system scheduled to arrive the following day.

At 0730 h on 23 January, we departed the dock and moved offshore to anchorage to make way for the RVIB *Nathaniel B. Palmer*. While at anchorage, we received the last remaining supplies necessary to sail. We were cleared by immigration and departed for the Amundsen Sea at 1418 h on 23 January. Because of significant weather and seas to the west, we took the eastern route through the Strait of Magellan. The total transit from Punta Arenas to the first proposed site (ASRE-09A) was ~1800 nmi. The pilot departed the ship at 2024 h on 23 January, and we exited the Strait of Magellan into the South Atlantic shortly after. Late in the day of 24 January, we departed the Atlantic Ocean through the Le Maire Strait, which is the passage between the Argentine portion of Tierra del Fuego and Isla de los Estados; entered the Southern Ocean; and started heading southwest toward the Amundsen Sea.

At the start of our transit, ice and weather data indicated that none of the continental shelf sites and only a few of the continental rise sites could be occupied, and forecasts led us to aim for Proposed Site ASRE-09A. During our transit, evolving data, forecasts, and science priorities led us to change our first site to Proposed Site ASRE-08A, which is ~33 nmi east of Proposed Site ASRE-09A. After a transit of 1770 nmi over 7.3 days at an average speed of 10.1 nmi/h, we arrived at Site U1532 at 2100 h on 30 January.

Site U1532

We conducted operations in 7 holes at Site U1532 (Table **T1**). We cored in 5 holes, collectively recovering core from the seafloor to 787.41 m (Holes U1532A–U1532D and U1532G) with an overall recovery of 90%. Two holes penetrated substantially into the seafloor but had to be abandoned before coring could start because of approaching ice (Holes U1532E and U1532F). We spent a total of 23.7 days at Site U1532. Drifting icebergs caused multiple interruptions that resulted in nearly half of this time (11.46 days) being spent waiting for ice to clear the area or performing operations not originally planned (pipe trips, reentries, or repeated drilled intervals). The frequency of interruptions caused by drifting icebergs and significant variations in their speed and direction proved problematic. In Hole U1532G, deployment of a free-fall reentry system shortly after starting to drill into the seafloor allowed us to core to 787 m.

Hole U1532A

We arrived at Site U1532 at 2100 h on 30 January. We lowered the thrusters, switched to dynamic positioning mode at 2145 h, and began drill floor operations. After assembling the outer core barrel and spacing out the inner core barrel, we started assembling and lowering the bottom-hole assembly (BHA) to the seafloor. On 31 January, we finished assembling the remaining drill collars and spent the first half of the day lowering the drill string to the seafloor and verifying the internal diameter clearance and length of each piece of the drill string. At 1200 h on 31 January, we installed the top drive and pumped two pigs down through the drill string to clean the inside of the drill pipe before coring. After adjusting the bit to 3968.6 m below the rig floor, we installed the APC core orientation tool, lowered the APC core barrel, and started coring in Hole U1532A at 1650 h on 31 January.

Core 1H recovered 5.63 m, resulting in a seafloor depth of 3961.5 mbsl. Cores 1H through 11H penetrated from 0 to 100.6 m and recovered 103.04 m (102%). All APC cores were oriented, and formation temperature measurements were made with the advanced piston corer temperature tool (APCT-3) coring shoe while taking Cores 4H (34.0 m), 7H (62.6 m), and 10H (91.1 m). After recovering Core 11H, we had to stop coring at 0645 h on 1 February because of a combination of approaching ice and increasing difficulty observing ice caused by fog and snow and a slight swell. We raised the bit to 50 m with the intention of resuming coring in Hole U1532A after conditions improved. Instead, we pulled the bit out of the hole at 0930 h on 1 February, raised the bit 100 m above the seafloor, and spent until 0015 h on 2 February adjusting our position to maintain a safe distance from ice. Although we had a free-fall funnel (FFF) readied for deployment, we did not deploy it given the balance between the time it would take to deploy the FFF and reenter it compared to the time it would take to redrill to 100 m in a new hole and resume coring from there.

Hole U1532B

After the drill floor was cleared to resume operations, we offset the ship 20 m to the east of Hole U1532A and started drilling in Hole U1532B at 0125 h on 2 February. We drilled from the seafloor to 93.1 m without coring, recovered the XCB core barrel with a center bit, and started APC coring. The first core in Hole U1532B (Core 2H) arrived on the rig floor at 0415 h on 2 February. While we were taking the next core (3H), we had to pause coring again because of approaching ice. We raised the bit to 50.5 m and waited for the ice to clear from 0800 to 1515 h. We then resumed APC coring, and Core 4H (112.1–121.6 m with a formation temperature measurement) arrived on deck at 1800 h. Before it was laid out on the rig floor, approaching ice forced us to stop coring again. We raised the bit to 50.5 m and waited from 1830 to 2215 h on 2 February before being able to lower the bit to the bottom of the hole and resume coring at 2300 h.

We continued APC coring and recovered Cores 5H through 9H (121.6–169.1 m with a formation temperature measurement on Core 7H). After recovering Core 9H, approaching ice forced us to pause coring again at 0600 h on 3 February, and the bit was raised to 50.5 m. We were able to resume operations at 0900 h, so we lowered the bit to 169.1 m and resumed coring. Core 10H was a partial stroke with the lowermost core liner deformed and a crack extending up the entire core liner. Core 10H recovered 6.48 m, so we advanced the bit 6.5 m and switched to HLAPC coring. After Core 11F (175.6–180.3 m) was recovered, approaching ice once again forced us to pause coring at 1315 h on 3 February, and we had to raise the bit to 50.5 m. Unfortunately, the ice kept converging on our location, so we eventually had to pull the bit completely out of the hole at 1715 h on 3 February. Once again, we decided not to deploy a FFF and opted instead to drill to 180 m in the next hole and resume coring from that depth. We spent the rest of the 3 February positioning the ship to avoid the drifting ice. Overall, Hole U1532B was drilled without coring from the seafloor to 93.1 m. APC/HLAPC coring penetrated 87.2 m (93.1–180.3 m) and recovered 91.9 m (105%).

Hole U1532C

At 0000 h on 4 February, we were able to resume operations. The ship was offset 20 m to the south of Hole U1532B, and at 0035 h on 4 February we started drilling into the seafloor in Hole U1532C. We drilled without coring from the seafloor to 178.3 m by 0415 h. After retrieving the core barrel with the center bit used during the drilling, we started HLAPC coring. Core 2F (178.3–183.0 m) arrived on deck at 0630 h. This core was positioned to overlap with the deepest core in Hole U1532B (Core 11F; 175.6–180.3 m). Cores 2F through 11F (178.3–225.3 m) were recovered, but approaching ice forced us to pause coring at ~1630 h on 4 February. The barrel for Core 12F had already been deployed and had to be recovered before we raised the bit to 61.9 m. We received the approval to resume operations at 1900 h on 4 February, so we lowered the bit to the bottom of the hole and resumed HLAPC coring. After Cores 12F through 18F penetrated from 225.3 to 258.2 m, we switched to the XCB system. Cores 19X through 22X penetrated from 258.2 to 291.0 m (10.18 m recovered; 31%), after which Cores 20X and 21X only recovered 6 cm. At 1445 h on 5 February, as Core 22X arrived at the rig floor, approaching ice forced us to pause coring and raise the bit to 50.5 m. We were able to resume operations at 1715 h on 5 February. After lowering the bit to the bottom of the hole, we took Cores 23X and 24X (291.0–310.1 m; 18.05 m recovered, 95%).

Just as Core 24X arrived on the rig floor at 2355 h on 5 February, we had to stop coring again and raise the bit to 50.5 m because of approaching ice. At 0530 h on 6 February, we resumed operations and started lowering the bit to the bottom of the hole. The bit encountered a bridge in the hole at 172.5 m, so we deployed an XCB core barrel with a center bit to drill through it and then washed the bit down to the bottom of the hole at 310.1 m. We circulated 25 bbl of mud to clean cuttings out of the hole and retrieved the center bit to resume XCB coring. Just as we were about to drop the XCB barrel to start coring, approaching ice put operations on hold again. This time, however, we kept the bit near the bottom of the hole. At 1545 h on 6 February, the ice moved away and we resumed XCB coring. After Cores 25X through 33X penetrated from 310.1 to 392.3 m, approaching ice and diminishing visibility caused by snow forced us to pause coring, and Core 33X was pulled after only penetrating 5.5 m. At this point, we decided to abandon further XCB coring and switch to RCB coring because

- Penetrating deeply at this site was a primary objective and would require RCB coring,
- RCB coring may result in better quality core at the current hole depths, and
- We wanted to take advantage of the time spent waiting for ice and environmental conditions to improve.

We started recovering the drill string at 1315 h on 7 February. The bit cleared the seafloor at 1520 h, and we continued raising the drill string. Overall, Hole U1532C was drilled without coring from the seafloor to 178.3 m, and HLAPC/XCB coring penetrated 214.0 m (178.3–392.3 m) and recovered 179.6 m (84%). We did not consider deploying a FFF in Hole U1532C and opted to start a new hole instead because this would provide better chances of coring deeply with the RCB. Hole U1533C was drilled/cored with an 11⁷⁄₁₆ inch bit, and we had been in the hole for nearly 4.5 days; both factors contributed to an oversized uppermost top of the hole. Reusing this hole would have hampered our ability to core deeply with the smaller diameter RCB bit (9⅞ inches).

Hole U1532D

We finished recovering the drill string and the APC/XCB BHA with the bit arriving on the rig floor at 0045 h on 8 February. After laying out the APC/XCB-specific parts of the BHA (seal bore and nonmagnetic drill collars), the drill crew started putting together the RCB BHA. Some extra time was required to fix a couple of issues identified by the routine verification of the drill collar interior diameter and core barrel space out in the BHA. From 0700 to 1430 h on 8 February, we lowered the bit until it was 21.5 m above the seafloor. We then installed the top drive, deployed a center bit, and adjusted the drill string to prepare for starting Hole U1532D. We planned to start RCB coring at ~362 m to overlap with the deepest cores from Hole U1532C. Unfortunately, at 1545 h on 8 February we had to pause operations because of approaching ice. We maneuvered the ship to avoid the ice until it cleared the area. We were finally able to start drilling into the seafloor at 2142 h on 8 February. We drilled without coring to 247.2 m by 0730 h on 9 February. Unfortunately, at this time approaching ice forced us to raise the bit to 55.5 m. The rig floor was cleared to resume operations at 1530 h on 9 February, and we lowered the bit to the bottom of the hole. At 1715 h, we dropped an RCB core barrel with a center bit and resumed drilling from 247.2 m. At 2300 h on 9 February, the bit reached 362.7 m and we started to recover the center bit to prepare for RCB coring.

We deployed an RCB core barrel at 0000 h on 10 February and started RCB coring in Hole U1532D. After Cores 2R through 3R penetrated from 362.7 to 381.9 m, at 0415 h on 10 February approaching ice forced us to raise the bit to just below the seafloor. The ice kept converging, so we had to pull the bit completely out of Hole U1532D at 0605 h on 10 February. We did not have sufficient time to deploy a FFF before having to pull out of the hole. Overall, Hole U1532D was drilled without coring from the seafloor to 362.7 m, and RCB coring penetrated 19.2 m (362.7–381.9 m) and recovered 17.42 m (91%).

Hole U1532E and U1532F

Instead of waiting for the ice to pass and allow us to resume operations, we decided to move ~0.4 nmi to the northwest along the seismic reflection profile and start a new hole. After waiting until 1145 h for ice to clear the area, we started drilling without coring in Hole U1532E, and the bit reached 101.6 m at 1445 h on 10 February. Increasing winds, snow, and swell made it difficult to visually track smaller pieces of ice, which do not show clearly on the radar. This, combined with larger ice in the area, made us pause operations and raise the bit to just below the seafloor (48.6 m). Unfortunately, at 1830 h on 10 February approaching ice forced us to pull the bit completely out of Hole U1532E. Because we had not penetrated significantly and the ice was converging on our position quickly, we did not choose to deploy a FFF. We raised the bit to 105 m above the seafloor to wait for the ice to move out of the area. We took advantage of this downtime to conduct routine servicing of the drill line (slip and cut). We moved back to the location of Holes U1532A–U1532D and started drilling without coring in Hole U1532F at 2315 h on 10 February. We planned to start RCB coring at ~378 m, just above the maximum coring depth in Hole U1532D. We drilled without coring from the seafloor to 105.1 m, where we had to stop to fix a hydraulic hose in the top drive (0230–0430 h on 11 February). When the bit reached 321.4 m (at 1630 h on 11 February), approaching ice forced us to stop drilling, recover the RCB core barrel with the center bit, and raise the bit to just below the seafloor (45.5 m). Again, the ice was converging on our position too quickly to deploy a FFF. We pulled the bit out of seafloor at 1921 h on 11 February and waited for the ice to clear the area with the bit just above the seafloor.

Hole U1532G

At 0900 h on 12 February, we decided that because of the frequency of ice interruptions, a reentry system more substantial than a FFF would be required for the multiple reentries needed to core deeply. So, we removed the top drive and recovered the drill string, and the bit arrived on the rig floor at 1845 h on 12 February. While recovering the drill string, we started preparing the parts of a free-fall reentry system (casing shoe, one joint of casing, mud skirt, the outer structural parts of the hydraulic release tool, and FFF cone). As soon as the bit was on board, we spent the rest of the day assembling the reentry system in the center of the moonpool beneath the rig floor.

We completed assembling the free-fall reentry system at 0115 h on 13 February and then started lowering the RCB drilling assembly through the middle of the reentry system to the seafloor. After starting Hole U1532G at 0920 h and penetrating to 51.9 m, we dropped the reentry system at 1100 h on 13 February. We continued drilling without coring to 161.5 m but had to pause operations from 1730 to 1815 h because of approaching ice. After spending ~1 h clearing ice from the wireline seal (blowout preventer) in the top drive, we resumed drilling. When the bit reached 171.2 m at 1945 h on 13 February, approaching ice forced us to pause operations again and raise the bit to 54 m.

At 0345 h on 14 February, we had to pull completely out of Hole U1532G. At 0700 h on 14 February, we adjusted the bit depth for reentry, deployed the subsea camera system, and reentered Hole U1532G at 1005 h. We recovered the camera system and started lowering the drill string. When the bit reached 201.5 m at 1345 h, we had to raise the bit to 45.5 m because of approaching ice. After the rig floor was cleared to resume operations at 1630 h on 14 February, we lowered the bit to the bottom of the hole and resumed drilling without coring.

At 0345 h on 15 February, we reached the depth where we wanted to start coring (372.3 m). After clearing ice from the wireline seal in the top drive and sinker bars, we recovered the RCB core barrel with the attached center bit and started RCB coring. Once Core 3R arrived on deck, approaching ice forced us to pause operations at 1100 h. We resumed coring at 1330 h. After Core 14R (487.5–-497.1 m) arrived on the rig floor at 1315 h on 16 February, approaching ice forced us to stop coring. We raised the bit to 65 m and waited for the ice to clear the area. We resumed operations at 1845 h on 17 February, lowering the bit from 65.0 to 467.5 m and resuming RCB coring at 2130 h on 17 February. We then had nearly 40 h of uninterrupted coring. Cores 15R through 34R penetrated from 497.1 to 688.6 m and recovered 170.51 m (89%).

After Core 34R arrived at 1445 h on 19 February, we had to stop coring because of approaching ice. At 1915 h, we were able to resume coring, and Cores 35R through 37R penetrated another 28.7 m (688.6–717.3 m; 24.73 m recovered; 86%). As soon as we finished cutting Core 37R at 0045 h on 20 February, we had to raise the bit to 54.5 m because of approaching ice. We were finally able to retrieve Core 37R at 0420 h.

At ~0655 h on 20 February, we were cleared to resume coring and started lowering the bit down the hole. After we installed the top drive, the bit encountered some resistance at 567.5 m, and we rotated and circulated to 709.2 m. At that depth, we had to drop a center bit to redrill the final ~8 m to the bottom of the hole (709.2–717.3 m). After circulating 25 bbl of mud to clean the cuttings out of the hole, approaching ice forced us to raise the bit to 64.5 m at 1315 h. We continued waiting on ice to clear the area until 0230 h on 21 February, when approaching ice forced us to pull the bit out of Hole U1532G so that we could offset the ship. At 0630 h, we deployed the camera system in anticipation of being able to reenter Hole U1532G. After adjusting the bit depth for reentry at 0845 h, we surveyed the seafloor around Hole U1532G and began attempts to reenter the hole. The FFF of the reentry system (with ~14 m of casing below) was not visible; it had settled substantially into the seafloor. After numerous attempts, we were finally able to reenter at 1225 h. After we recovered the camera system, we started lowering the bit to the bottom of the hole. At 1615 h, the bit encountered some resistance at 620.5 m, so we installed the top drive so that we could circulate and rotate, dropped a core barrel, and reamed to the bottom of the hole (717.3 m). We recovered the core barrel (Core 38G; 0.47 m recovered) at 2125 h and resumed RCB coring. Cores 39R through 45R then penetrated from 717.3 to 779.9 m. Approaching ice forced us to stop cutting Core 45R after penetrating only 5.1 m. At 1315 h on 22 February, we raised the bit to 754.5 m and recovered Core 45R. We resumed operations at 1615 h, lowered the bit to the bottom of the hole, and started coring at 1700 h. After Cores 46R through 47R (779.9–787.41 m) were recovered, we paused operations again at 2245 h because of approaching ice and raised the bit to 64.5 m. We continued waiting on the ice to clear the area until 0545 h on 23 February, when the approaching ice forced us to pull the bit out of the hole. At 0630 h, we decided to stop further operations in Hole U1532G and started to recover the drill string. The bit arrived on the rig floor at 1335 h, and the rig floor was secured for transit at 1455 h. Before we could get under way, we had to maneuver the ship away from the ice to raise the thrusters. We started our transit to Site U1533 at 1618 h.

Overall, Hole U1532G was drilled without coring from the seafloor to 372.3 m and then cored with the RCB system from 372.3 to 794.0 m, recovering 366.41 m (87%).

Site U1533

We conducted coring operations in 4 holes at Site U1533 (Proposed Site ASRE-09A; Table **T1**). Given the frequent interruptions caused by icebergs at the previous site, we decided to deploy a free-fall reentry system as early as possible after starting to core. APC coring in Hole U1533A penetrated from the seafloor to 28.5 m and recovered 29.54 m (104%), but approaching ice forced us to pull out of the hole before deploying the reentry system. Hole U1533B was drilled without coring to 25.5 m, after which we cored to a total depth of 382.6 m with the APC, HLAPC, XCB, and RCB systems for overall recovery of 70%. Shortly after beginning APC coring in Hole U1533B, we deployed a free-fall reentry system with 24.35 m of 10¾ inch casing that allowed us to reenter the hole two times after we were driven off by approaching ice. The first time the ice forced us to pull out of Hole U1533B, we used the time to conduct shallow-penetration APC coring in Holes U1533C and U1533D before returning to Hole U1533B. Hole U1533C consisted of a single mudline core that recovered 7.74 m, but increased ship heave forced us to stop drilling operations. After the seas subsided, we conducted APC coring in Hole U1533D from the seafloor to 40.0 m and recovered 40.01 m (100%).

We spent a total of 11.68 days at Site U1533. Drifting icebergs caused multiple interruptions that resulted in nearly half of this time (5.22 days) being spent waiting for ice to clear the area or conducting operations not originally planned (pipe trips, reentries, or repeated drilled intervals). The frequency of interruptions caused by drifting icebergs and significant variations in their speed and direction proved problematic. We had to stop any further expedition drilling operations at 0315 h on 7 March 2019 to return to Chilean waters to evacuate an injured crew member.

Hole U1533A

After completing operations at Site U1532, we started our transit to Site U1533 at 1618 h on 23 February. After the 31 nmi transit (4.4 h; 7.1 nmi/h), we arrived at Site U1533 and switched to dynamic positioning at 2109 h. Once at the site, we conducted routine servicing of the drill line (slip and cut), prepared the rig floor and moonpool for assembling a reentry system, and then assembled the free-fall reentry system (FFF, mud skirt, 2 joints of 10¾ inch casing). At 0330 h on 24 February, the reentry system was completed and centered in the moonpool. We attached an APC bit to the BHA and lowered it through the reentry system. We used an APC polycrystalline diamond compact (PDC) bit, which has a smaller outside diameter (9⅞ inches) than our normal APC bits so that it can pass through the 10¾ inch casing used in the reentry system. While lowering the bit to the seafloor, we had to stop for 2 h (0800–1000 h) to repair a line in the rig floor compressed air system. After the bit arrived at ~90 m above the seafloor at 1500 h, we had to pause operations because of approaching ice. At 1715 h, we installed the top drive and adjusted the bit to start coring. Unfortunately, we had to stop operations again at 1930 h because of approaching ice.

After ice cleared the area at 0515 h on 25 February, we adjusted the bit depth and started APC coring in Hole U1533A at 0640 h. Cores 1H through 3H penetrated to 28.5 m and recovered 29.54 m (104%). Ice approached, and we had to pull out of Hole U1533A at 1045 h before being able to deploy the reentry system.

Hole U1533B (first visit)

We resumed operations at 1300 h on 25 February. We offset the ship ~1620 m to the west (264°) of Hole U1533A because the ice conditions would allow us to start operations sooner at this location, which is along the range of locations on the seismic profile approved for drilling at this site. Hole U1533B was started at 1355 h, and we drilled without coring to 25.5 m. APC Cores 2H through 7H then penetrated to 82.5 m. While retrieving Core 4H, we deployed the free-fall reentry system with 24.35 m of 10¾ inch casing.

After Core 7H arrived at the rig floor at 0050 h on 26 February, approaching ice caused us to pause operations and raise the bit to 50.4 m. We resumed operations at 0230 h, and Cores 8H through 12H penetrated to 130.0 m. After recovering Core 12H, approaching ice forced us to pause operations again at 1100 h, and the bit was raised to 50.6 m. At 1415 h, we lowered the bit to the bottom of the hole and resumed APC coring. Cores 13H through 18H penetrated to 187.0 m before we had to pause operations again 2330 h. We raised the bit to 50.6 m to wait for the ice to clear the area.

At 0330 h on 27 February, we had to pull completely out of Hole U1533B because of approaching ice. Because the ice encroachment would not allow the timely reentry of Hole U1533B, we decided to make use of this time to take a few surficial APC cores.

Holes U1533C and U1533D

We offset the ship to a more ice-free portion of the seismic profile and adjusted the bit for a mudline core. As we prepared to shoot Core 379-U1533C-1H at 0805 h, significant ship heave caused the core to fire early. However, we recovered what appeared to be a good, 7.7 m long mudline core. Before we could take any more cores, increasing ship heave forced us to stop operations at 0900 h on 27 February. We raised the bit ~100 m above the seafloor and waited until 0645 h on 28 February for the seas to subside enough to resume coring operations. Our preference was to reenter Hole U1533B and continue to deepen it, but this required calmer seas because we did not want to risk the bit heaving down on the reentry funnel and damaging our ability to reenter. So, we offset the ship 15 m to the east of Hole U1533C and started APC coring from the seafloor in Hole U1533D. APC Cores U1533D-1H through 5H penetrated to 40 m and recovered 40.01 m (100%). Because this was deep enough to provide overlap with the shallowest Hole U1533B cores and the swell had decreased enough to allow deeper drilling, we terminated Hole U1533D at 1545 h on 28 February.

Hole U1533B (second visit)

We moved back to Hole U1533B, deployed the camera system, and reentered at 1838 h on 28 February. The top of the reentry cone was observed to be roughly level with the seafloor but clear on all sides from a depression made by the 96 inch^2 mud skirt. We recovered the camera system and lowered the bit toward the bottom of the hole. The bit encountered some resistance at 160 m, so we installed the top drive and rotated/circulated the remaining 27 m to the bottom of the hole (187.0 m). We resumed coring at 2215 h, and Cores 19F and 20F penetrated to 196.4 m. After Core 20F arrived on the rig floor at 0055 h on 1 March, we had to stop coring because of approaching ice. At 0130 h, we raised the bit to 165.6 m, removed the top drive, and continued raising the bit to 50.6 m. At 0600 h, we resumed operations, lowered the bit to the bottom of the hole, and started coring again. After two HLAPC cores (21F and 22F; 196.4–205.8 m), we decided to switch to XCB coring. Unfortunately, we had to stop operations at 1115 h because of approaching ice. We raised the bit to 50.6 m and waited until 1515 h to resume operations. We lowered the bit to the bottom of the hole and drilled Cores 23X through 28X from 205.8 to 262.1 m. After Core 28X arrived on the rig floor, we had to stop operations at 0915 h on 2 March because of approaching ice. We raised the bit to 50.6 m and waited until 1315 h to resume operations. While lowering the bit to the bottom of the hole, it encountered hard fill at 232.6 m. We installed the top drive, deployed an XCB core barrel with a center bit, and drilled to 262.1 m. After recovering the center bit, we resumed coring at 1645 h, and Cores 29X through 31X penetrated to 283.9 m. At 2145 h, we had to stop coring again because of approaching ice. Instead of waiting for the ice to leave the area to resume XCB coring, we decided to make use of this time to retrieve the drill string and switch to RCB coring. We pulled the bit out of Hole U1533B at 2303 h and retrieved the drill string.

The APC/XCB bit arrived on the rig floor at 0820 h on 3 March. Core 31X was recovered with the drill string. We prepared the RCB BHA and lowered it the seafloor. We deployed the camera system to prepare for reentering Hole U1533B. During the deployment of the camera system, we attached the APCT-3 to the camera system to measure the seawater temperature from the surface to just above the seafloor. Once the camera system reached the bit, we adjusted the bit depth to reenter Hole U1533B, but approaching ice forced us to raise the bit to 70 m above the seafloor at 2045 h. We were cleared to resume operations at 2215 h and reentered Hole U1533B at 2305 h. We recovered the camera system and lowered the bit into Hole U1533B. After the camera system was on board, we installed the top drive and circulated and rotated to the bottom of the hole (283.9 m). Approaching ice prevented us from coring, causing a delay from 0315 to 0630 h on 4 March. Unfortunately, ice kept converging on our location, so we had to raise the bit to 66 m. At 1215 h, we resumed operations and lowered the bit toward the bottom of the hole. The bit encountered resistance at 257.6 m, and we had to drill to the bottom of the hole. At 1345 h, we started RCB coring from 283.9 m. Cores 32R through 35R then penetrated to 316.0 m but recovered only 0.07 m (0.2%). At 2245 h, we raised the bit to 65.5 m because of approaching ice.

After ice cleared the area at 0145 h on 5 March, we lowered the bit from 65.6 m down the hole. The bit encountered fill at 267.6 m, so we installed the top drive and circulated/rotated the rest of the way down. We resumed RCB coring from 316.0 m at 0415 h. Cores 36R through 38R then penetrated to 341.7 m before we had to stop coring again at 1130 h because of approaching ice. We raised the bit to 65.5 m, reinstalled the top drive, and recovered Core 38R at 1415 h. At 1845h, we were able to resume operations, so we lowered the bit down the hole, installed the top drive when the bit was at 324.6 m, and circulated/rotated to the bottom of the hole (341.7 m). We then cut Cores 39R and 40R to 360.9 m. Before we could recover Core 40R, approaching ice forced us to pause operations again at 2315 h. We waited for the ice to clear with the bit near the bottom of the hole. We did not install the core line to retrieve Core 40R because it would increase the time required to pull out of the hole if the ice kept approaching. At 0315 h on 6 March, we were finally able to recover Core 40R and resume coring. Cores 41R through 43R penetrated from 360.9 to 382.6 m. At 0930 h, approaching ice again forced us to raise the bit to 65.6 m. The ice kept approaching, and we had to pull the bit completely out of Hole U1533B at 1115 h. With the bit 106 m above the seafloor, we installed the top drive, installed the core line, and recovered Core 43R at 1300 h. We then deployed the camera system at 1330 h so that we would be ready to reenter Hole U1533B as soon as the ice would allow. While waiting for the ice to move away, we conducted a camera survey of the seafloor from 1845 to 2030 h.

We continued to wait with the bit 50 m above the seafloor for the ice to clear the area until 0100 h on 7 March. We then reentered Hole U1533B at 0155 h, started to retrieve the camera system, and began lowering the bit into the hole. When the bit reached 324.6 m at 0315 h, we had to stop any further operations so that we could return to Chilean waters to evacuate an injured crew member. After the camera system was on board at 0430 h, we recovered the drill string. The rig floor was secured for transit at 1330 h.

Transit to Punta Arenas

We began the ~1358 nmi transit to a point south of Cape Horn for the medical evacuation at 1448 h on 7 March. Poor visibility combined with ice in the area initially limited our speed to ~6–7 nmi/h through the morning of 8 March. After that, improved visibility and good weather and seas allowed us to proceed much faster with an overall average speed of 11.5 nmi/h for the ~1358 nmi transit.

As the transit progressed, the evacuation location changed to Puerto Williams, Chile. We reached the Cape Horn pilot station at 1400 h on 12 March, two pilots boarded at 1503 h, and we proceeded to Puerto Williams. At 0006 h on 13 March, we arrived in Puerto Williams and anchored. Chilean officials (agent, immigration, port authority, police, and translator) boarded at 0020 h and departed at 0045 h. Later that morning, the helicopter for the medical evacuation landed on the ship at 0816 h and departed at 0838 h with the injured crew member. At 1009 h, we departed Puerto Williams and spent the rest of the day in transit to Punta Arenas.

We arrived at the Mardones Dock in Punta Arenas at 2000 h on 14 March and went through immigration and customs. From 15 to 19 March, we conducted port call activities that included preparing shipments for offloading, loading and distributing incoming shipments, preparing the labs for the next expedition, and completing all shipboard reports. Expedition 379 officially ended at 0800 h on 20 March.

Outreach

Expedition 379 had two Education and Outreach officers on board the ship. One was a children's author and illustrator, an informal educator, and the creator of a weekly science comic, #AntarcticLog. The other was a geologist as well as a photographer, writer and filmmaker who tells expedition science stories in the media.

Live broadcasts

We worked precruise to book more than 50 live broadcasts with schools, universities, and museums all over the world including the Smithsonian Museum of Natural History and the Natural History Museum of London. Because of internet connectivity issues, most of these had to be canceled and were moved to future expeditions. We managed to conduct five live events when we had connectivity: fifth and sixth graders in New Jersey (USA), the University of Perpignan in France with the French media present, and one to IODP Germany's live outreach event for 600 school children, reaching approximately 680 people in total.

Expedition activities

The expedition was continually documented by the two outreach officers using film, photo, writing, and interviews. A total of 26 blogs were posted on the *JOIDES Resolution* website, including updates from the scientists, technicians, and outreach officers. In addition, four blogs by scientist Claus-Dieter Hillenbrand were edited and photos were provided for the British Antarctic Survey. Biweekly comics for #AntarcticLog were produced leading up to and during the expedition; these were distributed through social media and blogs and will be published in an education and outreach booklet for IODP. A book, *Arcticology/Antarcticology*, for middle graders, was researched and drafted. A trailer video was produced for the expedition and disseminated through social media and blogs. Filming and interviews were completed for a follow-up film about IODP Expedition 379 as well as for a short film commissioned by BBC Global News about the expedition. Filming was completed for a Brazilian IODP (CAPES) promotional video featuring scientist Marcelo Mota.

Media

We filmed video featuring Co-Chief Scientist Karsten Gohl for the German science TV show *Nano* on 3sat, broadcast on 20 February 2019. We also filmed media for French TV that will be broadcast at later date. Photos, interviews, and information were provided for two German news articles and two French news articles. Three US news articles came from press releases published. BBC Earth Instagram published a series of photos from the expedition with an explanation of what we were doing. The post reached an audience of over 2.1 million people and was liked by over 40,000 people. The BBC World Service radio interviewed Co-Chief Scientist Julia Wellner.

Social media

Daily postings were made on Facebook, Instagram, and Twitter beginning prior to the cruise, just after the new year. These postings featured comics, including translations of one comic into nine different languages; photographs; videos; and information postings about activities aboard. Social media statistics include 53 Facebook posts with 168,143 people reached and 205 new followers; 83 Tweets with 276,000 impressions and 133 new followers; and 46 Instagram posts with 3,764 total likes.

References

Acton, G.D., Guyodo, Y., and Brachfeld, S.A., 2002. Magnetostratigraphy of sediment drifts on the continental rise of West Antarctica (ODP Leg 178, Sites 1095, 1096, and 1101). *In* Barker, P.F., Camerlenghi, A., Acton, G.D., and Ramsay, A.T.S. (Eds.), *Proceedings of the Ocean Drilling Program, Scientific Results,* 178: College Station, TX (Ocean Drilling Program), 1–61. **https://doi.org/10.2973/odp.proc.sr.178.235.2002**

Alonso, B., Anderson, J.B., Diaz, J.I., and Bartek, L.R., 1992. Pliocene–Pleistocene seismic stratigraphy of the Ross Sea: evidence for multiple ice sheet grounding episodes. *In* Elliot, D.H. (Ed.), *Antarctic Research Series* (Volume 57): *Contributions to Antarctic Research III:* Washington DC (American Geophysical Union), 93–103. **https://agupubs.onlinelibrary.wiley.com/doi/10.1029/AR057p0093**

Anderson, J.B., and Bartek, L.R., 1992. Cenozoic glacial history of the Ross Sea revealed by intermediate resolution seismic reflection data combined with drill site information. *In* Kennett J.P., and Warnke D. (Eds.), *Antarctic Research Series* (Volume 56): *The Antarctic Paleoenvironment: A Perspective on Global Change: Part One:* Washington DC (American Geophysical Union), 231–263. **https://agupubs.onlinelibrary.wiley.com/doi/pdf/10.1029/AR056p0231**

Anderson, J.B., Warny, S., Askin, R.A., Wellner, J.S., Bohaty, S.M., Kirshner, A.E., Livsey, D.N., et al., 2011. Progressive Cenozoic cooling and the demise of Antarctica's last refugium. *Proceedings of the National Academy of Sciences of the United States of America,* 108(28):11356–11360. **https://doi.org/10.1073/pnas.1014885108**

Anderson, J.B., and Wellner, J.S. (Eds.), 2011. *Tectonic, Climatic, and Cryospheric Evolution of the Antarctic Peninsula:* Washington, DC (American Geophysical Union). **https://doi.org/10.1029/SP063**

Arneborg, L., Wåhlin, A.K., Björk, G., Liljebladh, B., and Orsi, A.H., 2012. Persistent inflow of warm water onto the central Amundsen shelf. *Nature Geoscience,* 5(12):876–880. **https://doi.org/10.1038/ngeo1644**

Arrigo, K.R., van Dijken, G.L., and Bushinsky, S., 2008. Primary production in the Southern Ocean, 1997–2006. *Journal of Geophysical Research: Oceans,* 113(C8):C08004. **https://doi.org/10.1029/2007JC004551**

Barker, P.F., and Camerlenghi, A., 2002. Glacial history of the Antarctic Peninsula from Pacific margin sediments. *In* Barker, P.F., Camerlenghi, A., Acton, G.D., and Ramsay, A.T.S. (Eds.), *Proceedings of the Ocean Drilling Program, Scientific Results,* 178: College Station, TX (Ocean Drilling Program), 1–40. **https://doi.org/10.2973/odp.proc.sr.178.238.2002**

Bart, P.J., 2001. Did the Antarctic ice sheets expand during the early Pliocene? *Geology,* 29(1):67–70. **https://doi.org/10.1130/0091-7613(2001)029<0067:DTAISE>2.0.CO;2**

Bart, P.J., and Anderson, J.B., 2000. Relative temporal stability of the Antarctic ice sheets during the late Neogene based on the minimum frequency of outer shelf grounding events. *Earth and Planetary Science Letters,* 182(3–4):259–272. **https://doi.org/10.1016/S0012-821X(00)00257-0**

Bart, P.J., Egan, D., and Warny, S.A., 2005. Direct constraints on Antarctic Peninsula Ice Sheet grounding events between 5.12 and 7.94 Ma. *Journal of Geophysical Research: Earth Surface,* 110(F4):F04008. **https://doi.org/10.1029/2004JF000254**

Bart, P.J., and Iwai, M., 2012. The overdeepening hyphothesis: how erosional modification of the marine-scape during the early Pliocene altered glacial dynamics on the Antarctic Peninsula's Pacific margin. *Palaeogeography, Palaeoclimatology, Palaeoecology,* 335–336:42–51. **https://doi.org/10.1016/j.palaeo.2011.06.010**

Bartek, L.R., Vail, P.R., Anderson, J.B., Emmet, P.A., and Wu, S., 1991. Effect of Cenozoic ice sheet fluctuations in Antarctica on the stratigraphic signature of the Neogene. *Journal of Geophysical Research: Solid Earth,* 96(B4):6753–6778. **https://doi.org/10.1029/90JB02528**

Bentley, M.J., 2010. The Antarctic palaeo record and its role in improving predictions of future Antarctic Ice Sheet change. *Journal of Quaternary Science,* 25(1):5–18. **https://doi.org/10.1002/jqs.1287**

Carter, A., Riley, T.R., Hillenbrand, C.-D., and Rittner, M., 2017. Widespread Antarctic glaciation during the late Eocene. *Earth and Planetary Science Letters,* 458:49–57. **https://doi.org/10.1016/j.epsl.2016.10.045**

Chow, J.M., and Bart, P.J., 2003. West Antarctic Ice Sheet grounding events on the Ross Sea outer continental shelf during the middle Miocene. *Palaeogeography, Palaeoclimatology, Palaeoecology,* 198(1–2):169–186. **https://doi.org/10.1016/S0031-0182(03)00400-0**

Cook, C.P., van de Flierdt, T., Williams, T., Hemming, S.R., Iwai, M., Kobayashi, M., Jimenez-Espejo, F.J., et al., 2013. Dynamic behaviour of the East Antarctic Ice Sheet during Pliocene warmth. *Nature Geoscience,* 6(9):765–769. **https://doi.org/10.1038/ngeo1889**

Cowan, E.A., Hillenbrand, C.-D., Hassler, L.E., and Ake, M.T., 2008. Coarse-grained terrigenous sediment deposition on continental rise drifts: a record of Plio–Pleistocene glaciation on the Antarctica Peninsula. *Palaeogeography, Palaeoclimatology, Palaeoecology,* 265(3–4):275–291. **https://doi.org/10.1016/j.palaeo.2008.03.010**

De Santis, L., Anderson, J.B., Brancolini, G., and Zayatz, I., 1997. Glaciomarine deposits on the continental shelf of Ross Sea, Antarctica. *In* Davies, T.A., Bell, T., Cooper, A.K., Josenhans, H., Polyak, L., Solheim, A., Stoker, M.S., and Stravers, J.A. (Eds.), *Glaciated Continental Margins: An Atlas of Acoustic Images*: London (Chapman & Hall), 110–113. **https://doi.org/10.1007/978-94-011-5820-6_41**

De Santis, L., Prato, S., Brancolini, G., Lovo, M., and Torelli, L., 1999. The eastern Ross Sea continental shelf during the Cenozoic: implications for the West Antarctic Ice Sheet development. *Global and Planetary Change,* 23(1–4):173–196. **https://doi.org/10.1016/S0921-8181(99)00056-9**

DeConto, R.M., and Pollard, D., 2003. Rapid Cenozoic glaciation of Antarctica induced by declining atmospheric CO_2. *Nature,* 421(6920):245–249. **https://doi.org/10.1038/nature01290**

DeConto, R.M., and Pollard, D., 2016. Contribution of Antarctica to past and future sea-level rise. *Nature,* 531(7596):591–597. **https://doi.org/10.1038/nature17145**

Dowdeswell, J.A., Evans, J., Ó Cofaigh, C., and Anderson, J.B., 2006. Morphology and sedimentary processes on the continental slope off Pine Island Bay, Amundsen Sea, West Antarctica. *Geological Society of America Bulletin*, 118(5–6):606–619. **https://doi.org/10.1130/B25791.1**

Ehrmann, W., Hillenbrand, C.-D., Smith, J.A., Graham, A.G.C., Kuhn, G., and Larter, R.D., 2011. Provenance changes between recent and glacial-time sediments in the Amundsen Sea Embayment, West Antarctica: clay mineral assemblage evidence. *Antarctic Science,* 23(5):471–486. **https://doi.org/10.1017/S0954102011000320**

Escutia, C., Bárcena, M.A., Lucchi, R.G., Romero, O., Ballegeer, A.M., Gonzalez, J.J., and Harwood, D.M., 2009. Circum-Antarctic warming events between 4 and 3.5 Ma recorded in marine sediments from the Prydz Bay (ODP Leg 188) and the Antarctic Peninsula (ODP Leg 178) margins. *Global and Planetary Change,* 69(3):170–184. **https://doi.org/10.1016/j.gloplacha.2009.09.003**

Eyles, N., Daniels, J., Osterman, L.E., and Januszczak, N., 2001. Ocean Drilling Program Leg 178 (Antarctic Peninsula): sedimentology of glacially influenced continental margin topsets and foresets. *Marine Geology,* 178(1–4):135–156. **https://doi.org/10.1016/S0025-3227(01)00184-0**

Fretwell, P., Pritchard, H.D., Vaughan, D.G., Bamber, J.L., Barrand, N.E., Bell, R., Bianchi, C., et al., 2013. Bedmap2: improved ice bed, surface and thickness datasets for Antarctica. *The Cryosphere,* 7(1):375–393. **https://doi.org/10.5194/tc-7-375-2013**

Gohl, K., Denk, A., Eagles, G., and Wobbe, F., 2013a. Deciphering tectonic phases of the Amundsen Sea Embayment shelf, West Antarctica, from a magnetic anomaly grid. *Tectonophysics,* 585:113–123. **https://doi.org/10.1016/j.tecto.2012.06.036**

Gohl, K., Freudenthal, T., Hillenbrand, C.-D., Klages, J., Larter, R., Bickert, T., Bohaty, S., et al., 2017. MeBo70 seabed drilling on a polar continental shelf: operational report and lessons from drilling in the Amundsen Sea Embayment of West Antarctica. *Geochemistry, Geophysics, Geosystems,* 18(11):4235–4250. **https://doi.org/10.1002/2017GC007081**

Gohl, K., Uenzelmann-Neben, G., Larter, R.D., Hillenbrand, C.-D., Hochmuth, K., Kalberg, T., Weigelt, E., Davy, B., Kuhn, G., and Nitsche, F.O., 2013b. Seismic stratigraphic record of the Amundsen Sea Embayment shelf from pre-glacial to recent times: evidence for a dynamic West Antarctic Ice Sheet. *Marine Geology,* 344:115–131. **https://doi.org/10.1016/j.margeo.2013.06.011**

Gradstein, F.M., Ogg, J.G., Schmitz, M.D., and Ogg, G.M. (Eds.), 2012. *The Geological Time Scale 2012:* Amsterdam (Elsevier). **https://doi.org/10.1016/C2011-1-08249-8**

Graham, A.G.C., Larter, R.D., Gohl, K., Dowdeswell, J.A., Hillenbrand, C.-D., Smith, J.A., Evans, J., Kuhn, G., and Deen, T., 2010. Flow and retreat of the Late Quaternary Pine Island-Thwaites palaeo-ice stream, West Antarctica. *Journal of Geophysical Research: Earth Surface,* 115(F3):F03025. **https://doi.org/10.1029/2009JF001482**

Graham, A.G.C., Larter, R.D., Gohl, K., Hillenbrand, C.-D., Smith, J.A., and Kuhn, G., 2009. Bedform signature of a West Antarctic palaeo-ice stream reveals a multi-temporal record of flow and substrate control. *Quaternary Science Reviews,* 28(25–26):2774–2793. **https://doi.org/10.1016/j.quascirev.2009.07.003**

Haywood, A.M., Chandler, M.A., Valdes, P.J., Salzmann, U., Lunt, D.J., and Dowsett, H.J., 2009. Comparison of mid-Pliocene climate predictions produced by the HadAM3 and GCMAM3 general circulation models. *Global and Planetary Change,* 66(3–4):208–224. **https://doi.org/10.1016/j.gloplacha.2008.12.014**

Hepp, D.A., Mörz, T., and Grützner, J., 2006. Pliocene glacial cyclicity in a deep-sea sediment drift (Antarctic Peninsula Pacific margin). *Palaeogeography, Palaeoclimatology, Palaeoecology,* 231(1–2):181–198. **https://doi.org/10.1016/j.palaeo.2005.07.030**

Hepp, D.A., Mörz, T., Hensen, C., Frederichs, T., Kasten, S., Riedinger, N., and Hay, W.W., 2009. A late Miocene–early Pliocene Antarctic deepwater record of repeated iron reduction events. *Marine Geology,* 266(1–4):198–211. **https://doi.org/10.1016/j.margeo.2009.08.006**

Hillenbrand, C.-D., and Cortese, G., 2006. Polar stratification: a critical view from the Southern Ocean. *Palaeogeography, Palaeoclimatology, Palaeoecology,* 242(3–4):240–252. **https://doi.org/10.1016/j.palaeo.2006.06.001**

Hillenbrand, C.-D., and Ehrmann, W., 2005. Late Neogene to Quaternary environmental changes in the Antarctic Peninsula region: evidence from drift sediments. *Global and Planetary Change,* 45(1–3):165–191. **https://doi.org/10.1016/j.gloplacha.2004.09.006**

Hillenbrand, C.-D., Fütterer, D.K., Grobe, H., and Frederichs, T., 2002. No evidence for a Pleistocene collapse of the West Antarctic Ice Sheet from continental margin sediments recovered in the Amundsen Sea. *Geo-Marine Letters,* 22(2):51–59. **https://doi.org/10.1007/s00367-002-0097-7**

Hillenbrand, C.-D., Kuhn, G., and Frederichs, T., 2009. Record of a mid-Pleistocene depositional anomaly in West Antarctic continental margin sediments: an indicator for ice-sheet collapse? *Quaternary Science Reviews,* 28(13–14):1147–1159. **https://doi.org/10.1016/j.quascirev.2008.12.010**

Hillenbrand, C.-D., Kuhn, G., Smith, J.A., Gohl, K., Graham, A.G.C., Larter, R.D., Klages, J.P., et al., 2013. Grounding-line retreat of the West Antarctic Ice Sheet from inner Pine Island Bay. *Geology,* 41(1):35–38. **https://doi.org/10.1130/G33469.1**

Hillenbrand, C.-D., Smith, J.A., Hodell, D.A., Greaves, M., Poole, C.R., Kender, S., Williams, M., et al., 2017. West Antarctic Ice Sheet retreat driven by Holocene warm water incursions. *Nature,* 547(7661):43–48. **https://doi.org/10.1038/nature22995**

Hochmuth, K., and Gohl, K., 2013. Glaciomarine sedimentation dynamics of the Abbot glacial trough of the Amundsen Sea Embayment shelf, West Antarctica. *In* Hambrey, M.J., Barker, P.F., Barrett, P.J., Bowman, V., Davies, B., Smellie, J.L., and Tranter, M. (Eds.), *Antarctic Palaeoenvironments and Earth-Surface Processes.* Geological Society Special Publication, 381:233–244. **https://doi.org/10.1144/SP381.21**

Holden, P.B., Edwards, N.R., Wolff, E.W., Lang, N.J., Singarayer, J.S., Valdes, P.J., and Stocker, T.F., 2010. Interhemispheric coupling, the West Antarctic Ice Sheet and warm Antarctic interglacials. *Climate of the Past,* 6(4):431–443. **https://doi.org/10.5194/cp-6-431-2010**

Hollister, C.D., and Craddock, C., 1976. Introduction, principal results—Leg 35, Deep Sea Drilling Project. *In* Hollister, C.D., Craddock, C., et al., *Initial Reports of the Deep Sea Drilling Project,* 35: Washington, DC (U.S. Government Printing Office), 5–14. **https://doi.org/10.2973/dsdp.proc.35.101.1976**

Hughes, T.J., 1981. The weak underbelly of the West Antarctic Ice Sheet. *Journal of Glaciology*, 27(97):518–525. **https://doi.org/10.3189/S002214300001159X**

Intergovernmental Panel on Climate Change, 2007. *Climate Change 2007: Synthesis Report. Contribution of Working Groups I, II and III to the Fourth Assessment Report of the Intergovernmental Panel on Climate Change*: Geneva (Intergovernmental Panel on Climate Change). **http://climate.calcommons.org/bib/climate-change-2007-synthesis-report-contribution-working-groups-i-ii-and-iii-fourth-assessment**

Intergovernmental Panel on Climate Change, 2013. Summary for policymakers. *In* Stocker, T.F., Qin, D., Plattner, G.-K., Tignor, M., Allen, S.K., Boschung, J., Nauels, A., Xia, Y., Bex, V., and Midgley, P.M. (Eds.), *Climate Change 2013: The Physical Science Basis. Contribution of Working Group I to the Fifth Assessment Report of the Intergovernmental Panel on Climate Change:* Cambridge, United Kingdom (Cambridge University Press), 3–29. **http://www.climatechange2013.org/images/report/WG1AR5_SPM_FINAL.pdf**

Intergovernmental Panel on Climate Change, 2018. Summary for policymakers. *In* Masson-Delmotte, V., Zhai, P., Pörtner, H.-O., Roberts, D., Skea, J., Shukla, P.R., Pirani, A., et al. (Eds.), *Global Warming of 1.5°C:* Geneva (Intergovernmental Panel on Climate Change). **https://www.ipcc.ch/site/assets/uploads/sites/2/2018/07/SR15_SPM_version_stand_alone_LR.pdf**

Jacobs, S., Giulivi, C., Dutrieux, P., Rignot, E., Nitsche, F., and Mouginot, J., 2013. Getz Ice Shelf melting response to changes in ocean forcing. *Journal of Geophysical Research: Oceans,* 118(9):4152–4168. **https://doi.org/10.1002/jgrc.20298**

Jacobs, S., Jenkins, A., Hellmer, H., Giulivi, C., Nitsche, F., Huber, B., and Guerrero, R., 2012. The Amundsen Sea and the Antarctic Ice Sheet. *Oceanography*, 25(3):154–163. **https://doi.org/10.5670/oceanog.2012.90**

Jacobs, S.S., Jenkins, A., Giulivi, C.F., and Dutrieux, P., 2011. Stronger ocean circulation and increased melting under Pine Island Glacier ice shelf. *Nature Geoscience,* 4(8):519–523. **https://doi.org/10.1038/ngeo1188**

Jakobsson, M., Anderson, J.B., Nitsche, F.O., Dowdeswell, J.A., Gyllencreutz, R., Kirchner, N., Mohammad, R., et al., 2011. Geological record of ice shelf break-up and grounding line retreat, Pine Island Bay, West Antarctica. *Geology,* 39(7):691–694. **https://doi.org/10.1130/G32153.1**

Jakobsson, M., Anderson, J.B., Nitsche, F.O., Gyllencreutz, R., Kirshner, A.E., Kirchner, N., O'Regan, M., Mohammad, R., and Eriksson, B., 2012. Ice sheet retreat dynamics inferred from glacial morphology of the central Pine Island Bay Trough, West Antarctica. *Quaternary Science Reviews,* 38:1–10. **https://doi.org/10.1016/j.quascirev.2011.12.017**

Jenkins, A., Dutrieux, P., Jacobs, S., Steig, E.J., Gudmundsson, G.H, Smith, J., and Heywood, K.J., 2016. Decadal ocean forcing and Antarctic Ice Sheet response: lessons from the Amundsen Sea. *Oceanography,* 29(4):58–69. **https://doi.org/10.5670/oceanog.2016.103**

Joughin, I., and Alley, R.B., 2011. Stability of the West Antarctic Ice Sheet in a warming world. *Nature Geoscience,* 4(8):506–513. **https://doi.org/10.1038/ngeo1194**

Joughin, I., Alley, R.B., and Holland, D.M., 2012. Ice-sheet response to oceanic forcing. *Science,* 338(6111):1172–1176. **https://doi.org/10.1126/science.1226481**

Joughin, I., Smith, B.E., and Medley, B., 2014. Marine ice sheet collapse potentially under way for the Thwaites Glacier Basin, West Antarctica. *Science,* 344(6185):735–738. **https://doi.org/10.1126/science.1249055**

Kim, T.W., Ha, H.K., Wåhlin, A.K., Lee, S.H., Kim, C.S., Lee, J.H., and Cho, Y.K., 2017. Is Ekman pumping responsible for the seasonal variation of warm circumpolar deep water in the Amundsen Sea? *Continental Shelf Research,* 132:38–48. **https://doi.org/10.1016/j.csr.2016.09.005**

Kirshner, A.E., Anderson, J.B., Jakobsson, M., O'Regan, M., Majewski, W., and Nitsche, F.O., 2012. Post-LGM deglaciation in Pine Island Bay, West Ant-

arctica. *Quaternary Science Reviews,* 38:11–26.
https://doi.org/10.1016/j.quascirev.2012.01.017

Klages, J.P., Kuhn, G., Hillenbrand, C.-D., Smith, J.A., Graham, A.G.C., Nitsche, F.O., Frederichs, T., Jernas, P.E., Gohl, K., and Wacker, L., 2017. Limited grounding-line advance onto the West Antarctic continental shelf in the easternmost Amundsen Sea Embayment during the last glacial period. *PLoS One,* 12(7):e0181593.
https://doi.org/10.1371/journal.pone.0181593

Konfirst, M.A., Scherer, R.P., Hillenbrand, C.-D., and Kuhn, G., 2012. A marine diatom record from the Amundsen Sea—insights into oceanographic and climatic response to the Mid-Pleistocene Transition in the West Antarctic sector of the Southern Ocean. *Marine Micropaleontology,* 92–93:40–51. **https://doi.org/10.1016/j.marmicro.2012.05.001**

Larter, R.D., Anderson, J.B., Graham, A.G.C., Gohl, K., Hillenbrand, C.-D., Jakobsson, M., Johnson, J.S., et al., 2014. Reconstruction of changes in the Amundsen Sea and Bellingshausen Sea sector of the West Antarctic Ice Sheet since the Last Glacial Maximum. *Quaternary Science Reviews,* 100:55–86. **https://doi.org/10.1016/j.quascirev.2013.10.016**

Larter, R.D., Graham, A.G.C., Gohl, K., Kuhn, G., Hillenbrand, C.-D., Smith, J.A., Deen, T.J., Livermore, R.A., and Schenke, H.-W., 2009. Subglacial bedforms reveal complex basal regime in a zone of paleo-ice stream convergence, Amundsen Sea Embayment, West Antarctica. *Geology,* 37(5):411–414. **https://doi.org/10.1130/G25505A.1**

Larter, R.D., Rebesco, M., Vanneste, L.E., Gamboa, L.A.P., and Barker, P., 1997. Cenozoic tectonic, sedimentary and glacial history of the continental shelf west of Graham Land, Antarctic Peninsula. *In* Cooper, A.K., Barker, P.F., and Brancolini, G. (Eds.), *Geology and Seismic Stratigraphy of the Antarctic Margin* (Part 2). Antarctic Research Series, 71:1–27.
https://doi.org/10.1029/AR071p0001

Le Masurier, W.E., and Rex, D.C., 1991. The Marie Byrd Land volcanic province and its relation to the Cainozoic West Antarctic rift system. *In* Tingey, R.J. (Ed.), *The Geology of Antarctica*. Oxford Monographs on Geology and Geophysics, 17:249–284.

Lindeque, A., Gohl, K., Henrys, S., Wobbe, F., and Davy, B., 2016a. Seismic stratigraphy along the Amundsen Sea to Ross Sea continental rise: a cross-regional record of pre-glacial to glacial processes of the West Antarctic margin. *Palaeogeography, Palaeoclimatology, Palaeoecology,* 443:183–202. **https://doi.org/10.1016/j.palaeo.2015.11.017**

Lindeque, A., Gohl, K., Wobbe, F., and Uenzelmann-Neben, G., 2016b. Preglacial to glacial sediment thickness grids for the Southern Pacific margin of West Antarctica. *Geochemistry, Geophysics, Geosystems,* 17(10):4276–4285. **https://doi.org/10.1002/2016GC006401**

Lloyd, A.J., Wiens, D.A., Nyblade, A.A., Anandakrishnan, S., Aster, R.C., Huerta, A.D., Wilson, T.J., Dalziel, I.W.D, Shore, P.J., and Zhao, D., 2015. A seismic transect across West Antarctica: evidence for mantle thermal anomalies beneath the Bentley Subglacial Trench and the Marie Byrd Land Dome. *Journal of Geophysical Research: Solid Earth,* 120(12):8439–8460. **https://doi.org/10.1002/2015JB012455**

Lowe, A.L., and Anderson, J.B., 2002. Reconstruction of the West Antarctic Ice Sheet in Pine Island Bay during the Last Glacial Maximum and its subsequent retreat history. *Quaternary Science Reviews,* 21(16–17):1879–1897. **https://doi.org/10.1016/S0277-3791(02)00006-9**

McKay, R., Browne, G., Carter, L., Cowan, E., Dunbar, G., Krissek, L., Naish, T., et al., 2009. The stratigraphic signature of the late Cenozoic Antarctic Ice Sheets in the Ross Embayment. *Geological Society of America Bulletin,* 121(11–12):1537–1561. **https://doi.org/10.1130/B26540.1**

McKay, R., Naish, T., Carter, L., Riesselman, C., Dunbar, R., Sjunneskog, C., Winter, D., et al., 2012. Antarctic and Southern Ocean influences on late Pliocene global cooling. *Proceedings of the National Academy of Sciences of the United States of America,* 109(17):6423–6428.
https://doi.org/10.1073/pnas.1112248109

Milillo, P., Rignot, E., Rizzoli, P., Scheuchl, B., Mouginot, J., Bueso-Bello, J., and Prats-Iraola, P., 2019. Heterogeneous retreat and ice melt of Thwaites Glacier, West Antarctica. *Science Advances,* 5(1):eaau3433.
https://doi.org/10.1126/sciadv.aau3433

Miller, K.G., Wright, J.D., Katz, M.E., Browning, J.V., Cramer, B.S., Wade, B.S., and Mizintseva, S.F., 2008. A view of Antarctic ice-sheet evolution from sea-level and deep-sea isotope changes during the Late Cretaceous–Cenozoic. *In* Cooper, A.K., Barrett, P.J., Stagg, H., Storey, B., Stump, E., Wise, W., and the 10th ISAES Editorial Team (Eds.), *Antarctica: A Keystone in a Changing World.* Proceedings of the 10th International Symposium on Antarctic Earth Sciences, 10:55–70.
https://pubs.usgs.gov/of/2007/1047/kp/kp06/of2007-1047kp06.pdf

Minzoni, R.T., Majewski, W., Anderson, J.B., Yokoyama, Y., Fernandez, R., and Jakobsson, M., 2017. Oceanographic influences on the stability of the Cosgrove ice shelf, Antarctica. *The Holocene,* 27(11):1645–1658.
https://doi.org/10.1177/0959683617702226

Muto, A., Peters, L.E., Gohl, K., Sasgen, I., Alley, R.B., Anandakrishnan, S., and Riverman, K.L., 2016. Subglacial bathymetry and sediment distribution beneath Pine Island Glacier ice shelf modeled using aerogravity and in situ geophysical data: new results. *Earth and Planetary Science Letters,* 433:63–75. **https://doi.org/10.1016/j.epsl.2015.10.037**

Naish, T.R., Powell, R., Levy, R., Wilson, G., Scherer, R., Talarico, F., Krissek, L., et al., 2009. Obliquity-paced Pliocene West Antarctic Ice Sheet oscillations. *Nature,* 458(7236):322–329.
https://doi.org/10.1038/nature07867

Nitsche, F.O., Cunningham, A.P., Larter, R.D., and Gohl, K., 2000. Geometry and development of glacial continental margin depositional systems in the Bellingshausen Sea. *Marine Geology,* 162(2–4):277–302.
https://doi.org/10.1016/S0025-3227(99)00074-2

Nitsche, F.O., Gohl, K., Larter, R.D., Hillenbrand, C.-D., Kuhn, G., Smith, J.A., Jacobs, S., Anderson, J.B., and Jakobsson, M., 2013. Paleo ice flow and subglacial meltwater dynamics in Pine Island Bay, West Antarctica. *The Cryosphere,* 7(1):249–262. **https://doi.org/10.5194/tc-7-249-2013**

Nitsche, F.O., Gohl, K., Vanneste, K., and Miller, H., 1997. Seismic expression of glacially deposited sequences in the Bellingshausen and Amundsen Seas, West Antarctica. *In* Cooper, A.K., Barker, P.F., and Brancolini, G. (Eds.), *Geology and Seismic Stratigraphy of the Antarctic Margin* (Part 2). Antarctic Research Series, 71:95–108.
https://doi.org/10.1029/AR071p0095

Nitsche, F.O., Jacobs, S.S., Larter, R.D., and Gohl, K., 2007. Bathymetry of the Amundsen Sea continental shelf: implications for geology, oceanography, and glaciology. *Geochemistry, Geophysics, Geosystems,* 8(10):Q10009.
https://doi.org/10.1029/2007GC001694

Padman, L., Fricker, H.A., Coleman, R., Howard, S., and Erofeeva, L., 2002. A new tide model for the Antarctic ice shelves and seas. *Annals of Glaciology,* 34:247–254. **https://doi.org/10.3189/172756402781817752**

Pagani, M., Liu, Z., LaRiviere, J., and Ravelo, A.C., 2010. High Earth-system climate sensitivity determined from Pliocene carbon dioxide concentrations. *Nature Geoscience,* 3:27–30. **https://doi.org/10.1038/ngeo724**

Paolo, F.S., Fricker, H.A., and Padman, L., 2015. Volume loss from Antarctic ice shelves is accelerating. *Science,* 348(6232):327–331.
https://doi.org/10.1126/science.aaa0940

Parkinson, C.L., and Cavalieri, D.J., 2012. Antarctic sea ice variability and trends, 1979–2010. *The Cryosphere,* 6(4):871–880.
https://doi.org/10.5194/tc-6-871-2012

Passchier, S., Browne, G., Field, B., Fielding, C.R., Krissek, L.A., Panter, K., Pekar, S.F., and ANDRILL-SMS Science Team, 2011. Early and middle Miocene Antarctic glacial history from the sedimentary facies distribution in the AND-2A drill hole, Ross Sea, Antarctica. *Geological Society of America Bulletin,* 123(11–12):2352–2365.
https://doi.org/10.1130/B30334.1

Pollard, D., and DeConto, R.M, 2009. Modelling West Antarctic Ice Sheet growth and collapse through the past five million years. *Nature,* 458(7236):329–332. **https://doi.org/10.1038/nature07809**

Powell, R.D., and Cooper, J.M., 2002. A glacial sequence stratigraphic model for temperate, glaciated continental shelves. *In* Dowdeswell, J.A., and Ó'Cofaigh, C. (Eds.), *Glacier-Influenced Sedimentation on High-Latitude Continental Margins.* Geological Society Special Publication, 203:215–244. **https://doi.org/10.1144/GSL.SP.2002.203.01.12**

Rignot, E., Mouginot, J., Scheuchl, B., van den Broeke, M., van Wessem, M.J., and Morlighem, M., 2019. Four decades of Antarctic Ice Sheet mass balance from 1979–2017. Proceedings of the National Academy of Sciences.
https://doi.org/10.1073/pnas.1812883116

Rocchi, S., LeMasurier, W.E., and Di Vincenzo, G., 2006. Oligocene to Holocene erosion and glacial history in Marie Byrd Land, West Antarctica, inferred from exhumation of the Dorrel Rock intrusive complex and from volcano morphologies. *Geological Society of America Bulletin,* 118(7–8):991–1005. **https://doi.org/10.1130/B25675.1**

Scherer, R.P., 2003. Quaternary interglacials and the West Antarctic Ice Sheet. *In* Droxler, A.W., Poore, R.Z., and Burckle, L.H. (Eds.), *Earth's Climate and Orbital Eccentricity: The Marine Isotope Stage 11 Question*. Geophysical Monograph, 137:103–112. **https://doi.org/10.1029/137GM08**

Scherer, R.P., Aldahan, A., Tulaczyk, S., Possnert, G., Engelhardt, H., and Kamb, B., 1998. Pleistocene collapse of the West Antarctic Ice Sheet. *Science,* 281(5373):82–85. **https://doi.org/10.1126/science.281.5373.82**

Scheuer, C., Gohl, K., and Eagles, G., 2006a. Gridded isopach maps from the South Pacific and their use in interpreting the sedimentation history of the West Antarctic continental margin. *Geochemistry, Geophysics, Geosystems,* 7(11):Q11015. **https://doi.org/10.1029/2006GC001315**

Scheuer, C., Gohl, K., Larter, R.D., Rebesco, M., and Udintsev, G., 2006b. Variability in Cenozoic sedimentation along the continental rise of the Bellingshausen Sea, West Antarctica. *Marine Geology,* 277(3–4):279–298. **https://doi.org/10.1016/j.margeo.2005.12.007**

Schoof, C., 2007. Ice sheet grounding line dynamics: steady states, stability, and hysteresis. *Journal of Geophysical Research: Earth Surface,* 112(F3):F03S28. **https://doi.org/10.1029/2006JF000664**

Smellie, J.L., Haywood, A.M., Hillenbrand, C.-D., Lunt, D.J., and Valdes, P.J., 2009. Nature of the Antarctic Peninsula Ice Sheet during the Pliocene: geological evidence and modelling results compared. *Earth-Science Reviews,* 94(1–4):79–94. **https://doi.org/10.1016/j.earscirev.2009.03.005**

Smith, J.A., Andersen, T.J., Shortt, M., Gaffney, A.M., Truffer, M., Stanton, T.P., Bindschadler, R., et al., 2017. Sub-ice-shelf sediments record history of twentieth-century retreat of Pine Island Glacier. *Nature,* 541(7635):77–80. **https://doi.org/10.1038/nature20136**

Smith, J.A., Hillenbrand, C.-D. Kuhn, G., Klages, J.P., Graham, A.G.C., Larter, R.D., Ehrmann, W., Moreton, S.G., Wiers, S., and Frederichs, T., 2014. New constraints on the timing of West Antarctic Ice Sheet retreat in the eastern Amundsen Sea since the Last Glacial Maximum. *Global and Planetary Change,* 122:224–237. **https://doi.org/10.1016/j.gloplacha.2014.07.015**

Smith, J.A., Hillenbrand, C.-D., Kuhn, G., Larter, R.D., Graham, A.G.C., Ehrmann, W., Moreton, S.G., and Forwick, M., 2011. Deglacial history of the West Antarctic Ice Sheet in the western Amundsen Sea Embayment. *Quaternary Science Reviews,* 30(5–6):488–505. **https://doi.org/10.1016/j.quascirev.2010.11.020**

Smith, R.T., and Anderson, J.B., 2010. Ice-sheet evolution in James Ross Basin, Weddell Sea margin of the Antarctic Peninsula: the seismic stratigraphic record. *Geological Society of America Bulletin,* 122(5–6):830–842. **https://doi.org/10.1130/B26486.1**

Spiegel, C., Lindow, J., Kamp, P.J.J., Meisel, O., Mukasa, S., Lisker, F., Kuhn, G., and Gohl, K., 2016. Tectonomorphic evolution of Marie Byrd Land—implications for Cenozoic rifting activity and onset of West Antarctic glaciation. *Global and Planetary Change*, 145:98–115. **https://doi.org/10.1016/j.gloplacha.2016.08.013**

Sutter, J., Gierz, P., Grosfeld, K., Thoma, M., and Lohmann, G., 2016. Ocean temperature thresholds for Last Interglacial West Antarctic Ice Sheet collapse. *Geophysical Research Letters,* 43(6):2675–2682. **https://doi.org/10.1002/2016GL067818**

Thoma, M., Jenkins, A., Holland, D., and Jacobs, S., 2008. Modelling Circumpolar Deep Water intrusions on the Amundsen Sea continental shelf, Antarctica. *Geophysical Research Letters,* 35(18):L18602. **https://doi.org/10.1029/2008GL034939**

Uenzelmann-Neben, G., and Gohl, K., 2012. Amundsen Sea sediment drifts: archives of modifications in oceanographic and climatic conditions. *Marine Geology,* 299–302:51–62. **https://doi.org/10.1016/j.margeo.2011.12.007**

Uenzelmann-Neben, G., and Gohl, K., 2014. Early glaciation already during the early Miocene in the Amundsen Sea, Southern Pacific: indications from the distribution of sedimentary sequences. *Global and Planetary Change,* 120:92–104. **https://doi.org/10.1016/j.gloplacha.2014.06.004**

Uenzelmann-Neben, G., Gohl, K., Larter, R.D., and Schlüter, P., 2007. Differences in ice retreat across Pine Island Bay, West Antarctica, since the Last Glacial Maximum: indications from multichannel seismic reflection data. *In* Cooper, A.K., Raymond, C.R., et al. (Eds.), *Antarctica: A Keystone in a Changing World—Online Proceedings of the 10th International Symposium on Antarctic Earth Sciences.* USGS Open-File Report 2007-1047, Short Research Paper 084. **https://pubs.usgs.gov/of/2007/1047/srp/srp084/of2007-1047srp084.pdf**

Vaughan, D.G., 2008. West Antarctic Ice Sheet collapse—the fall and rise of a paradigm. *Climate Change,* 91(1–2):65–79. **https://doi.org/10.1007/s10584-008-9448-3**

Villa, G., Persico, D., Wise, S.W., and Gadaleta, A., 2012. Calcareous nannofossil evidence for Marine Isotope Stage 31 (1 Ma) in Core AND-1B, ANDRILL McMurdo Ice Shelf Project (Antarctica). *Global and Planetary Change,* 96–97:75–86. **https://doi.org/10.1016/j.gloplacha.2009.12.003**

Walker, D.P., Brandon, M.A., Jenkins, A., Allen, J.T., Dowdeswell, J.A., and Evans, J., 2007. Oceanic heat transport onto the Amundsen Sea shelf through a submarine glacial trough. *Geophysical Research Letters,* 34(2):L02602. **https://doi.org/10.1029/2006GL028154**

Warny, S., Askin, R.A., Hannah, M.J., Mohr, B.A.R., Raine, J.I., Harwood, D.M., Florindo, F., and the SMS Science Team, 2009. Palynomorphs from a sediment core reveal a sudden remarkably warm Antarctica during the middle Miocene. *Geology,* 37(10):955–958. **https://doi.org/10.1130/G30139A.1**

Weigelt, E., Gohl, K., Uenzelmann-Neben, G., and Larter, R.D., 2009. Late Cenozoic ice sheet cyclicity in the western Amundsen Sea Embayment—evidence from seismic records. *Global and Planetary Change,* 69(3):162–169. **https://doi.org/10.1016/j.gloplacha.2009.07.004**

Wellner, J.S., Lowe, A.L., Shipp, S.S., and Anderson, J.B., 2001. Distribution of glacial geomorphic features on the Antarctic continental shelf and correlation with substrate: implications for ice behavior. *Journal of Glaciology,* 47(158):397–411. **https://doi.org/10.3189/172756501781832043**

Wilch, T.I., McIntosh, W.C., and Dunbar, N.W., 1999. Late Quaternary volcanic activity in Marie Byrd Land: potential $^{40}Ar/^{39}Ar$-dated time horizons in West Antarctic ice and marine cores. *Geological Society of America Bulletin,* 111(10):1563–1580. **https://doi.org/10.1130/0016-7606(1999)111<1563:LQVAIM>2.3.CO;2**

Wilson, D.S., Jamieson, S.S., Barrett, P.J., Leitchenkov, G., Gohl, K., and Larter, R.D., 2012. Antarctic topography at the Eocene-Oligocene boundary. *Palaeogeography, Palaeoclimatology, Palaeoecology,* 335–336:24–34. **https://doi.org/10.1016/j.palaeo.2011.05.028**

Wilson, D.S., and Luyendyk, B.P., 2009. West Antarctic paleotopography estimated at the Eocene–Oligocene climate transition. *Geophysical Research Letters,* 36(16):L16302. **https://doi.org/10.1029/2009GL039297**

Wilson, D.S., Pollard, D., DeConto, R.M., Jamieson, S.S.R., and Luyendyk, B.P., 2013. Initiation of the West Antarctic Ice Sheet and estimates of total Antarctic ice volume in the earliest Oligocene. *Geophysical Research Letters,* 40(16):4305–4309. **https://doi.org/10.1002/grl.50797**

Table T1. Expedition 379 hole summary. — = no data.

Hole	Proposed site	Latitude	Longitude	Water depth (m)	Cored interval (m)	Core recovery (m)	Core recovery (%)	Drilled interval without coring (m)	Total penetration (m)	Time in hole (h)	Time in hole (days)
U1532A	ASRE-08A	68° 38.6833′S	107° 31.5003′W	3961.5	100.6	103.04	102	—	100.6	35.75	1.5
U1532B		68° 36.6837′S	107° 31.4696′W	3961.4	87.2	91.92	105	93.1	180.3	55.75	2.3
U1532C		68° 36.6952′S	107° 31.4721′W	3961.4	214.0	179.60	84	178.3	392.3	103.50	4.3
U1532D		68° 36.6953′S	107° 31.5015′W	3961.5	19.2	17.42	91	362.7	381.9	53.25	2.2
U1532E		68° 36.4292′S	107° 32.4613′W	3977.4	—	—	—	101.6	101.6	12.50	0.5
U1532F		68° 36.6833′S	107° 31.5303′W	3961.4	—	—	—	321.4	321.4	48.25	2.0
U1532G		68° 36.6954′S	107° 31.5299′W	3961.4	421.7	366.41	87	372.3	794.0	260.25	10.8
				Site U1532 totals:	842.7	758.39	90	1429.4	2272.1	569.25	23.7
U1533A	ASRE-09A	68° 44.0168′S	109° 0.6014′W	4180.8	28.5	29.54	104	—	28.5	37.50	1.6
U1533B		68° 44.0994′S	109° 3.0010′W	4190.1	357.1	250.78	70	25.5	382.6	206.50	8.6
U1533C		68° 44.0696′S	109° 1.5103′W	4183.1	7.7	7.74	101	—	7.7	4.50	0.2
U1533D		68° 44.0727′S	109° 1.4901′W	4183.9	40.0	40.01	100	—	40.0	31.75	1.3
				Site U1533 totals:	433.3	328.07	76	25.5	458.8	280.25	11.7
				Expedition 379 totals:	1276.0	1086.46	85	1454.9	2730.9	849.50	35.4

Figure F1. Eastern Amundsen Sea continental shelf and rise bathymetry. Red stars mark Expedition 379 sites on Resolution Drift (RD), which is one of five large north-northeast–striking sediment drift bodies on the rise. Green circles show the location of Proposal 839 primary and alternate drill sites. Gray lines show the location of existing seismic lines. Annotated glacial troughs on the shelf are Dotson-Getz Trough (DGT), Pine Island Trough West (PITW), Pine Island Trough East (PITE), Pine Island Trough Central (PITC), and Abbot Trough (AT).

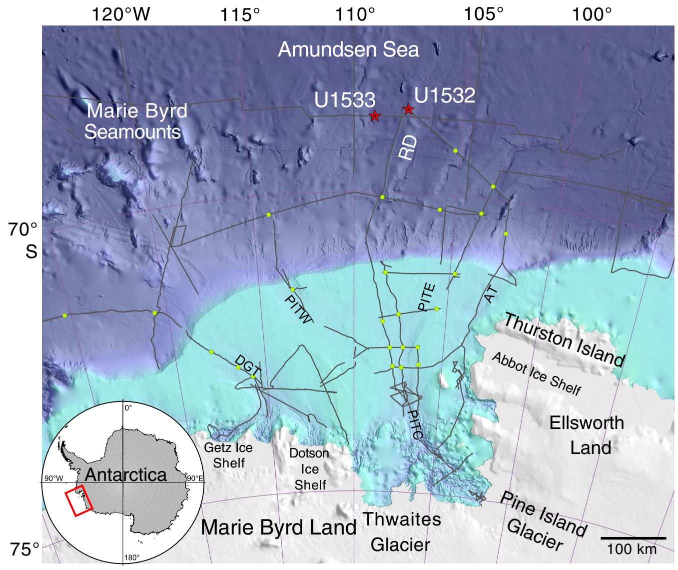

Figure F2. Antarctic ice sheet models for the Pliocene (modified from DeConto and Pollard, 2016) and the Last Interglacial (modified from Sutter et al., 2016) simulating the collapse of the West Antarctic Ice Sheet (WAIS) in both warm times. Major ice retreat in the Amundsen Sea Embayment (ASE) seems to be a precursor for partial or total WAIS collapse. EAIS = East Antarctic Ice Sheet.

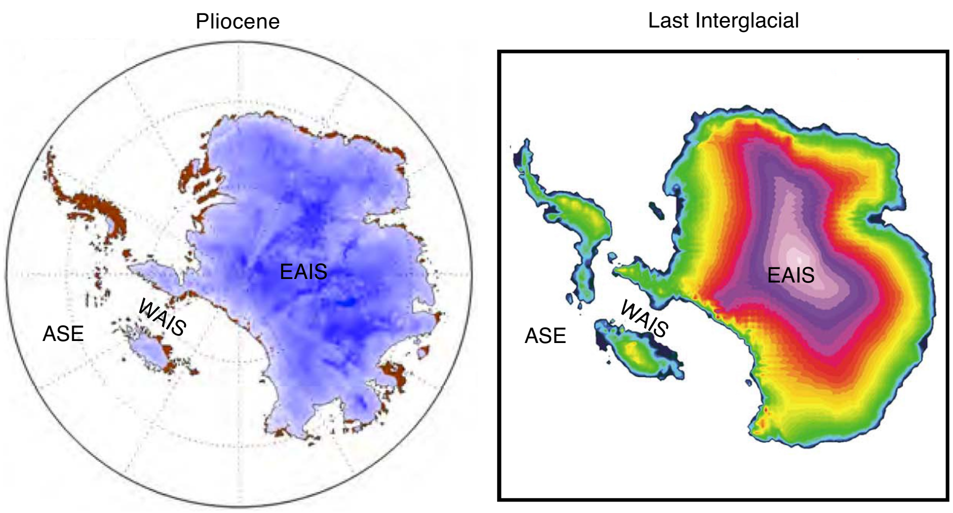

Figure F3. Seismic profile across continental rise of the eastern Amundsen Sea, with interpreted major sedimentary units and boundaries of a sediment drift system (modified from Uenzelmann-Neben and Gohl, 2014). CDP = common depth point.

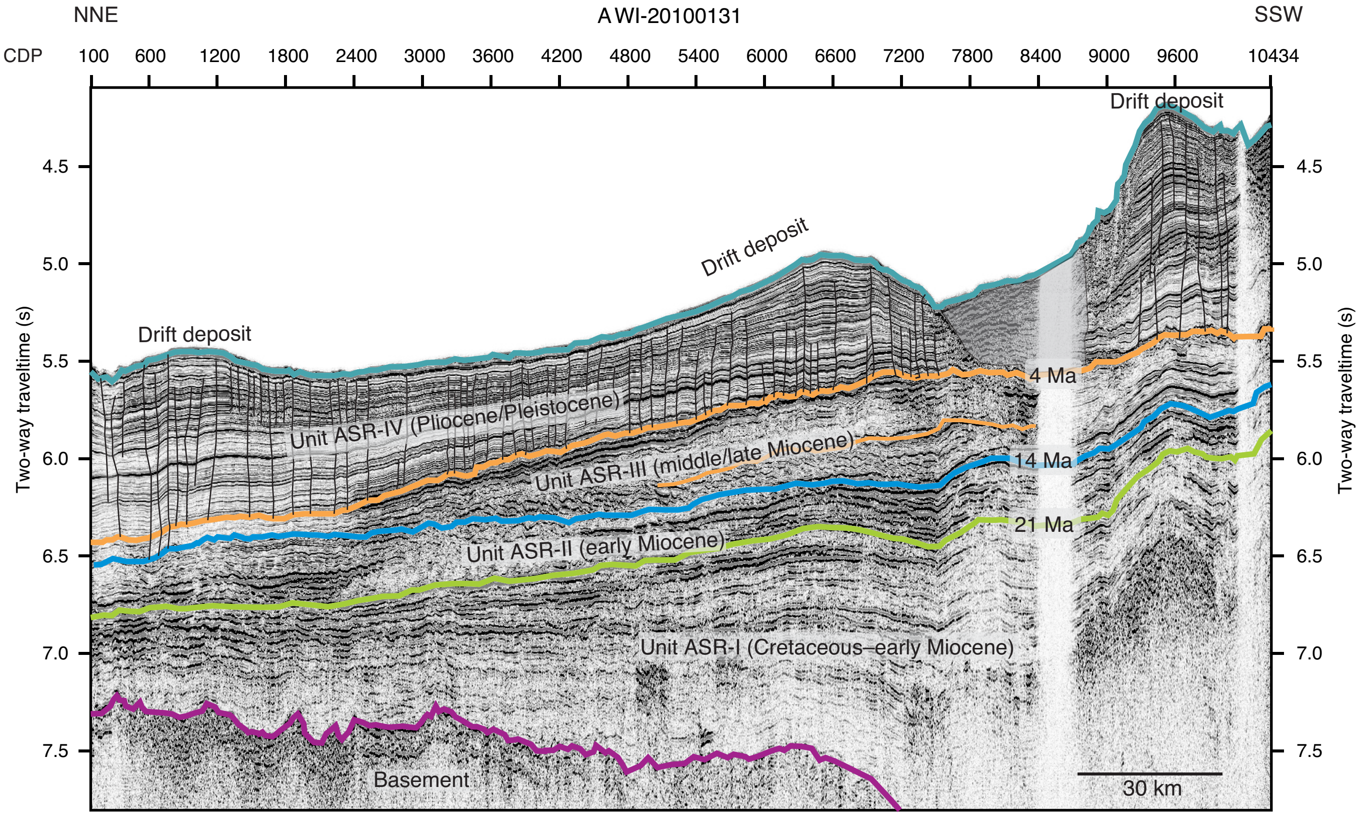

Figure F4. Site U1532 on the northwestern segment of Seismic Line AWI-20100130 that crosses Resolution Drift. Seismic horizons at the bases of the Pleistocene and Pliocene were preliminarily identified from the core records. Estimated age of the horizon at the base of Unit ASR-II is from Uenzelmann-Neben and Gohl (2014). CDP = common depth point.

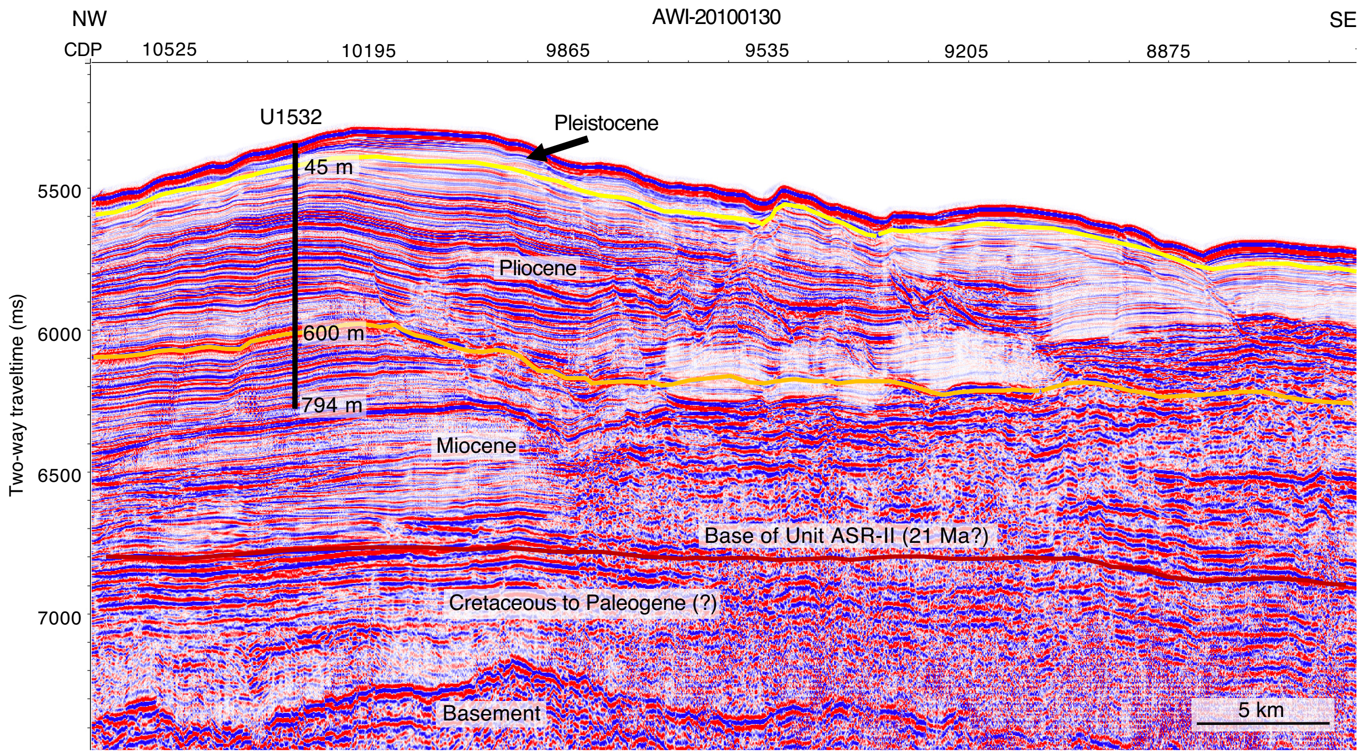

Figure F5. Hole U1532A–U1532G locations.

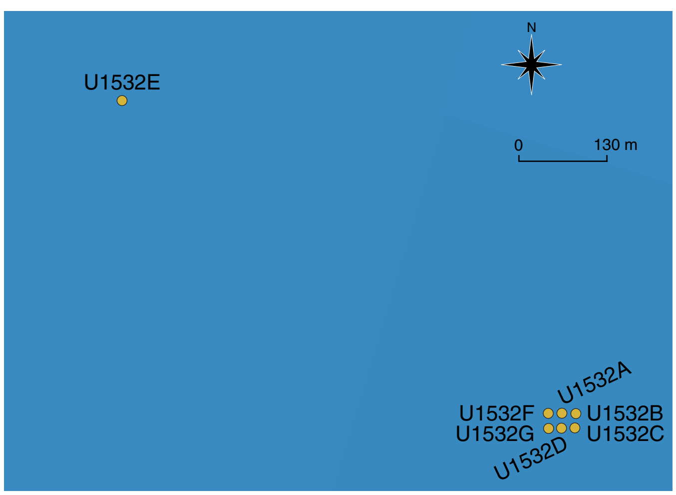

Figure F6. Site U1533 on Seismic Line TH86003B at the lowermost western flank of Resolution Drift. Seismic horizons at the bases of the Pleistocene and Pliocene were preliminarily identified from the core records. Estimated age of the horizon at the base of Unit ASR-II is from Uenzelmann-Neben and Gohl (2012). CDP = common depth point.

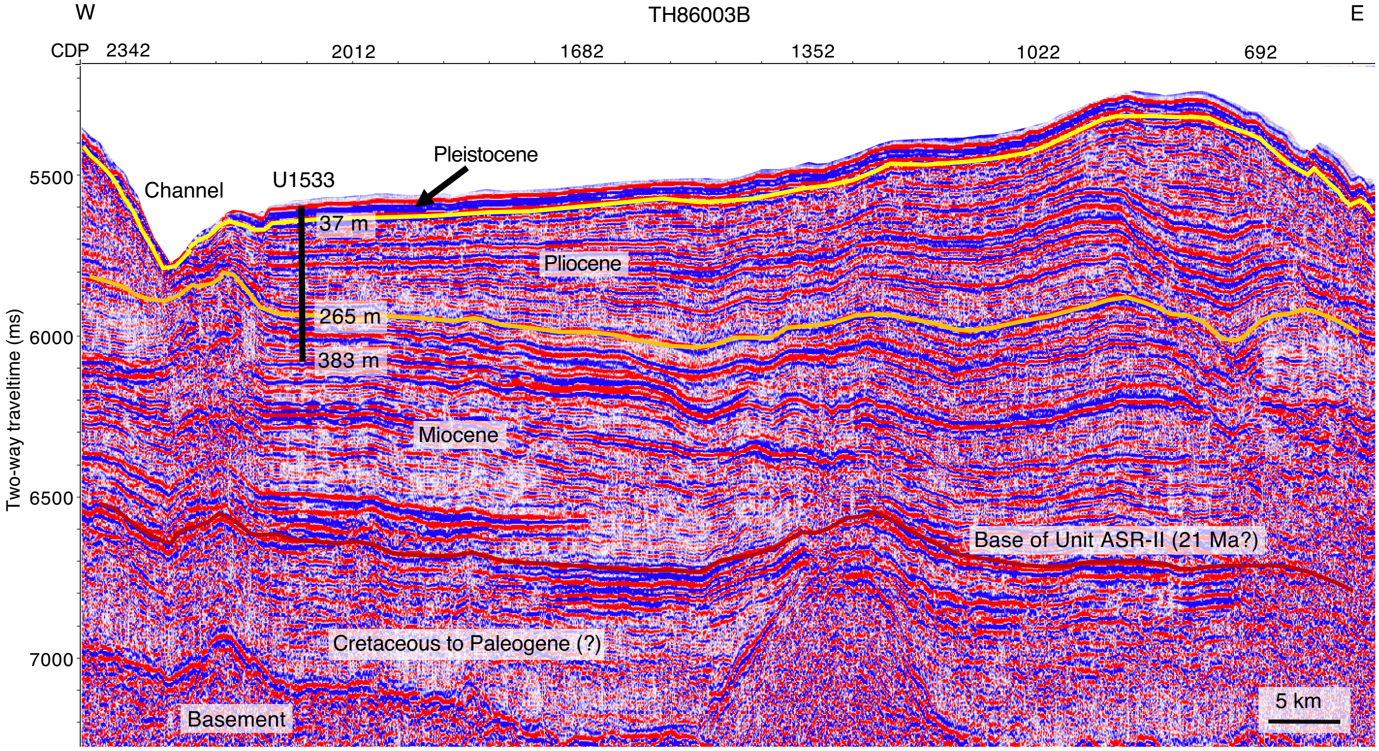

Figure F7. Hole U1533A–U1533D locations.

Figure F8. Composite lithostratigraphic summary, Holes U1532A–U1532D and U1532G. Lithostratigraphic subunits are divided based on changes in facies assemblages.

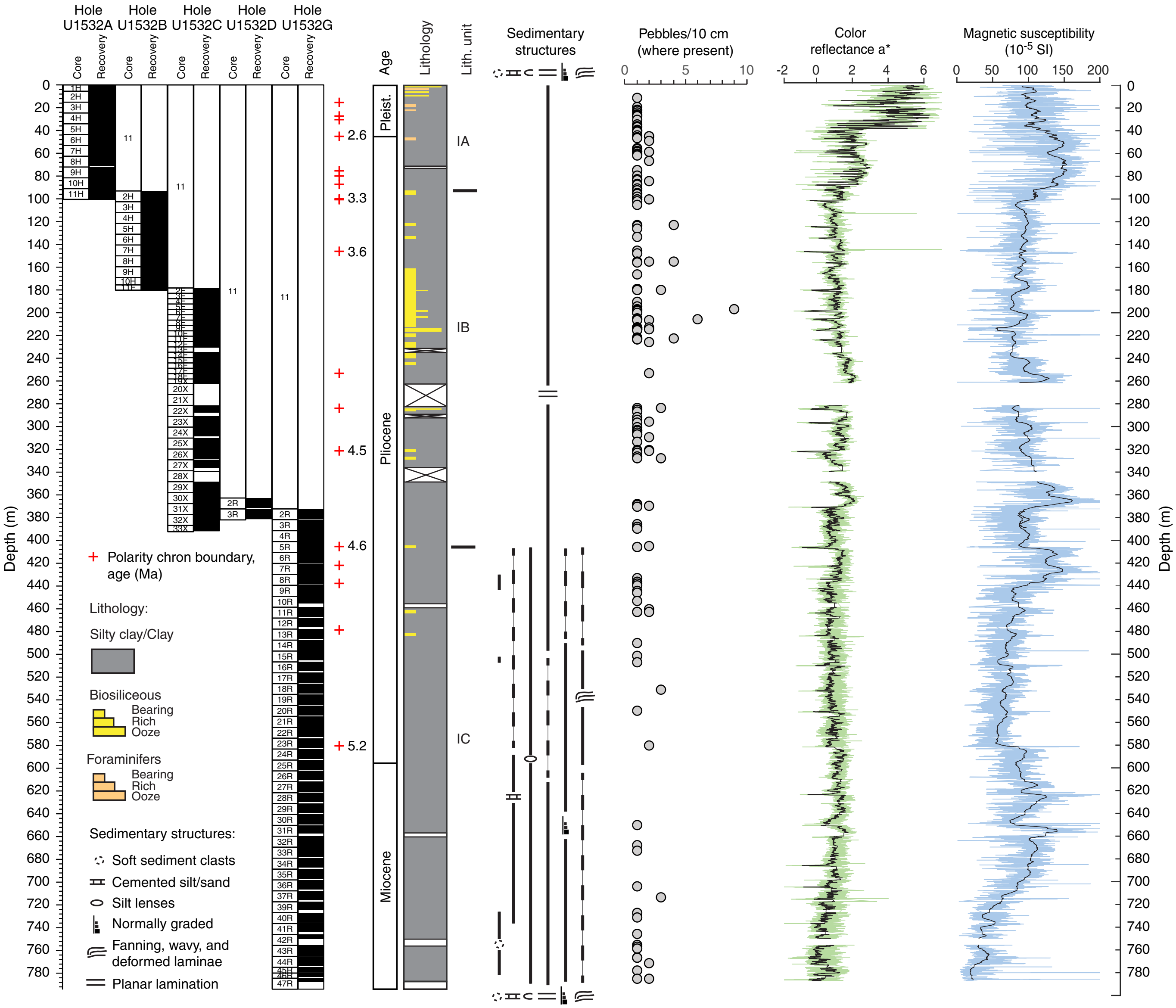

Figure F9. omposite lithostratigraphic summary, Holes U1533A–U1533D. Lithostratigraphic subunits are divided based on changes in facies assemblages.